

# Carbon Nanotubes as Carriers in Drug Delivery for Non-Small Cell Lung Cancer, Mechanistic Analysis of Their Carcinogenic Potential, Safety Profiling and Identification of Biomarkers

Zhongjian Pu<sup>1,\*</sup>, Yujia Wei<sup>2,3,\*</sup>, Yuanpeng Sun<sup>1</sup>, Yajun Wang<sup>1</sup>, Shilin Zhu<sup>1</sup>

<sup>1</sup>Department of Oncology, Haian Hospital of Traditional Chinese Medicine, Haian, 216600, People's Republic of China; <sup>2</sup>School of Medicine, Yangzhou University, Yangzhou, 225009, People's Republic of China; <sup>3</sup>Department of General Practice, Suzhou Wuzhong Hospital of Traditional Chinese Medicine, Suzhou, 215101, People's Republic of China

\*These authors contributed equally to this work

Correspondence: Yajun Wang; Shilin Zhu, Department of Oncology, Haian Hospital of Traditional Chinese Medicine, Haian, 216600, People's Republic of China, Email wangyajunhaian@21cn.com; zhushilinhaian@tom.com

**Abstract:** Non-small cell lung cancer (NSCLC) is a global burden leading to millions of deaths worldwide every year. Nanomedicine refers to the use of materials at the nanoscale for drug delivery and subsequent therapeutic approaches in cancer. Carbon nanotubes (CNTs) are widely used as nanocarriers for therapeutic molecules such as plasmids, siRNAs, antisense agents, aptamers and molecules related to the immunotherapy for several cancers. They are usually functionalized and loaded with standard drug molecules to improve their therapeutic efficiency. Functionalization and drug loading possibly decrease the genotoxic and carcinogenic potential of CNTs. In addition, the targeted cytotoxic properties of the drug improve and undesired toxicity decreases after drug loading and/or conjugation with proteins, including antibodies. For intended drug delivery, a lysosomal pH of 5.5 is more suitable and effective for the slow and extended release of cytotoxic drugs than a physiological pH 7.4. Remarkably, CNTs possess intrinsic antitumor properties and are usually internalized by endocytosis. After being internalized, several mechanisms are involved in the therapeutic and carcinogenic effects of CNTs. They are generally safe for therapy, and their toxicity profile remains dependent on their physicochemical properties. Moreover, the dose, route, duration of exposure, surface properties and degradative potential determine the toxicity outcomes of CNTs locally or systemically. In summary, the use of CNTs in drug delivery and NSCLC therapy, as well as their genotoxic and carcinogenic potential and the possible mechanisms, has been discussed in this review. The therapeutic index is generally high for NSCLC cells treated with drug-loaded CNTs; therefore, they are effective carriers in implementing targeted therapy for NSCLC.

**Keywords:** NSCLC, CNTs, drug delivery, antitumor, carcinogenic

## Introduction

Diseases of the cardiovascular system, persistent respiratory disorders, malignant cancers and diabetes constitute the noncommunicable disease burden.<sup>1</sup> As a global burden, these diseases account for 40 million deaths every year, which is equivalent to nearly three-quarters of the total deaths worldwide, among which cancers account for 16%.<sup>2</sup> Accordingly, the World Health Organization (WHO) plans to decrease this global burden by reducing the use of tobacco and alcohol dependence considerably before 2030. The goals of the WHO also aim to provide unbiased access to clinical care that includes prevention and curative treatment for both acute and chronic disorders.<sup>3</sup>

Cancer has become the leading cause of mortality worldwide, and the estimates are transitioning throughout China recently towards a higher incidence compared with the USA. In this regard, 4.82 million new cases and 3.21 million deaths are estimated for 2022 in China.<sup>4</sup> Lung cancer is the leading cause of deaths among cancers, accounting for 350 deaths every day in the USA alone. According to the American Cancer Society estimate, 236,740 new cases and 130,180 deaths are projected

for the year 2022.<sup>5</sup> Lung cancer includes a group of tumors that originate in the parenchyma or bronchi of the lungs.<sup>6</sup> Additionally, this cancer is broadly classified into two types, small cell (SCLC) and non-small cell lung cancers (NSCLCs), which account for 13% and 83% of cases based on the specificity of the treatment, respectively, whereas the remaining cases remain unclassified.<sup>7</sup> NSCLC remains a widely acknowledged cause of cancer-deaths, and its unique characteristics make this type of cancer difficult to understand and treat.<sup>8</sup>

Nanotechnology and the nanoaspired materials are in high global demand and projections between 2020 and 2027 claim that this demand will rise at a rate of 13% every year. As the global estimate for 2019 was 8500 million USD, the revenue projections for 2030 are set at 30,000 billion USD. The applications of nanotechnology in medicine and related sectors are key contributors to this growing market across countries including China.<sup>9</sup> Related to the goals of the WHO in disease prevention and cure for noncommunicable diseases, nano medicine is a growing field with investments increasing in health care every year. Interestingly, anticancer medications based on nanomaterials accounted for more than 30% of the global nanomedicine market in 2014.<sup>10</sup> However, due to several reasons including safety testing issues, inconclusive guidelines and lack of benefits, nanomedicine is still in its early phases and has not yet reached a developed stage.<sup>11</sup>

Nanomaterials are extensively used in diagnosing, visualizing and treating tumors of the lung at the primary or distant sites after metastasizing.<sup>12</sup> Among such nanomaterials, CNTs are deemed to be prospective candidates as biosensors and for therapeutic approaches, delivery of potent cytotoxic agents, and diagnosis. They possess a high surface area, contact surfaces appropriate for effective drug loading, higher stability and biocompatibility, which can assist in targeted therapy at extended sites.<sup>13</sup> They are usually synthesized by chemical vapor deposition, electric arc discharge and laser ablation and are isolated by capillary electrophoresis and size exclusion chromatography. Several spectroscopic techniques including, Fourier transform infrared spectroscopy, X-ray photoelectron spectroscopy, X-ray diffraction and electron microscopy techniques, are employed in the characterization of CNTs.<sup>14</sup>

Single-walled carbon nanotubes (SWCNTs) are composed of a single layer of graphene folded into a tube-like structure.<sup>15</sup> Interestingly, multi-walled carbon nanotubes (MWCNTs) constitute multiple layers of graphene folded uniformly one above the other and are typically larger than SWCNTs. The average internal diameters of SWCNTs (~1 nm) vary with MWCNTs (5 to 20 nm). Additionally, the SWCNTs are insoluble in aqueous media, whereas MWCNTs are partially soluble in water. In addition to SWCNTs and MWCNTs, double-walled and functionalized CNTs are considered as other classes of CNTs.<sup>16,17</sup>

Microtubules are extremely dynamic structures comprising tubulin heterodimers and remain a key component of the cellular cytoskeleton. They can regulate cell migration, division and intracellular trafficking. Tubulin-binding chemotherapeutic drugs recognize these proteins as targets, leading to mitotic arrest and death of such malignant cells.<sup>18</sup> CNTs are chemically stable across different environments and behave as “smart” materials closely related to the mechanical behavior of microtubules (resilient tubular structures capable of forming larger bundles).<sup>19</sup> The advantage of using anticancer drug-loaded CNTs for cancer therapy is that the CNTs interact with microtubules biomimetically and result in an enhanced antitumor response of the drug *in vitro* and in animal models.<sup>20</sup>

With this background, the present review will focus on the opportunities for drug delivery and NSCLC therapy using CNTs, which are mechanisms involved in such effects by analyzing a series of *in vitro* and *in vivo* studies conducted at the preclinical level. In addition, the toxicity of CNTs at the genomic level, their oncogenic potential and the possible mechanisms are presented. The safety analysis for CNTs and methods to improve their therapeutic potential are also discussed.

## Cytotoxic Effects of Drug-Loaded CNTs on NSCLC Cells *in vitro*

CNTs are considered effective carriers for therapeutic molecules and cytotoxic drugs that can inhibit DNA replication and cell division. They are effectively used in gene therapy as carriers for plasmids, siRNAs, antisense agents and aptamers and are also used to carry immunotherapeutic agents. They are widely used in photodynamic therapy and photothermal therapy.<sup>21,22</sup> They are also used in the diagnosis of malignancies associated with the breast, blood, liver, pancreas and reproductive organs, as well as glioblastoma.<sup>23</sup> CNTs are usually functionalized at the surface or ends to expand their solubility and biocompatibility. This can provide them with the ability to improve intracellular targeting of the nucleus, cytoplasm and mitochondria. The modified CNTs can enhance the efficacy of the antitumor drugs they are conjugated with over a limited dose range and exhibit limited toxic effects toward noncancerous cells.<sup>24</sup>

## Cytotoxic Effects of MWCNTs

First, MWCNTs functionalized with  $-\text{COOH}$  were acylated using thionyl chloride and conjugated with bromocriptine. The diameters of these materials were 25 to 40 nm, while the lengths were  $\sim 500$  nm. The CNTs conjugated with the dopamine type 2 agonist were less toxic to MRC5 fibroblasts ( $\text{IC}_{50}$  of 250.2  $\mu\text{g}/\text{ml}$ ) than to A549 cells ( $\text{IC}_{50}$  of 49.20  $\mu\text{g}/\text{ml}$ ) after 24 hours. These values were reduced to 209.3 (MRC5) and 27.79  $\mu\text{g}/\text{ml}$  (A549) after 48 h of incubation. The apoptotic rate was 89.85% in A549 cells, whereas, in MRC5 cells, it was only 11.77%. The expression levels of the dopamine receptors DRD2 and DRD4 were significantly higher in CNT-treated cancer cells than in normal MRC5 cells. Protein expression studies revealed that the proapoptotic protein Bax was upregulated, whereas the antiapoptotic protein Bcl-2 was downregulated in CNT-treated A549 cells compared with MRC5 cells treated with CNTs.<sup>25</sup> Similarly, MWCNTs functionalized with naringenin possessed an average diameter of  $9.6 \pm 1.4$  nm and released naringenin effectively at pH 7.4 (83.5%) compared with pH 5.5 (60.8%) after 9 h compared with relatively smaller durations. The naringenin-functionalized CNTs presented limited cytotoxic effects on normal hFB fibroblasts compared with A549 cells. The concentrations required for 50% cell death of hFB cells and A549 cells were  $172.3 \pm 12.9$   $\mu\text{g}/\text{mL}$  and  $82.6 \pm 7.3$   $\mu\text{g}/\text{mL}$ , respectively.<sup>26</sup>

As mitochondrial targeting is critical in tumor therapy, CNTs coated with polyethylene glycol and loaded with the Bcl-2 inhibitor ABT737 were prepared with lengths of 250 to 400 nm. The uptake of CNTs into cancer cells remained dependent on clathrin-mediated endocytosis. The release of ABT737 (50%) was effective and occurred well before 288 h under acidic conditions (pH 5.0) related to the cancer cell environment. Under hematological conditions, the release was very slow ( $<10\%$  drug released before 30 h). The changes in mitochondrial membrane potential were significant in A549 cells treated with CNTs compared with free ABT737. ABT737-loaded CNTs exhibited higher inhibitory effects toward Bcl-2 and promoted the expression of Bax with elevated reactive oxygen species (ROS) and release of cytochrome C. Furthermore, the CNTs activated apoptosis in A549 cells compared with normal NHFB cells.<sup>27</sup> Likewise, MWCNTs conjugated with transferrin, surface functionalized with the  $\alpha$ -tocopherol derivative TPGS and loaded with docetaxel (40–50 nm in length and 150–200 nm wide) were 136-fold cytotoxic ( $0.32 \pm 0.01$   $\mu\text{g}/\text{ml}$ ) against A549 cells compared with free docetaxel ( $43.92 \pm 2.3$   $\mu\text{g}/\text{ml}$ ), as evidenced by the  $\text{IC}_{50}$  values. The CNTs entrapped docetaxel at  $74.9 \pm 2.4\%$  and released the drug steadily up to 72 h after which the release was  $25.33 \pm 0.6\%$ . Considerably higher volumes of A549 cells were undergoing apoptosis at sub-G1 phase via transferrin receptor-mediated endocytosis after treatment with CNTs.<sup>28</sup>

Supporting the results of the abovementioned studies, MWCNTs with lengths of 1 to 2  $\mu\text{m}$  and diameters of 20 to 30 nm were functionalized with amines, conjugated with hyaluronic acid and loaded with doxorubicin. The characteristics of the CNTs changed after functionalization and drug loading. The lengths decreased to 0.3 to 0.8  $\mu\text{m}$ , whereas the diameters increased, as observed through SEM (60 to 80 nm) and TEM (20 to 30 nm). The differences in particle characteristics were due to the fact that functionalized coatings are barely recognized by TEM compared with SEM. The average particle size increased from  $172.8 \pm 4.2$  nm for oxidized CNTs to  $451.3 \pm 8.7$  nm for drug-loaded CNTs. The drug release after 32 hours was 14.26% at pH 7.4, while the doxorubicin release was 36.50% at pH 5.5 after 24 hours. The dose-dependent cytotoxic effects of the CNTs on A549 cells were dependent on CD44-mediated endocytosis. The  $\text{IC}_{50}$  of the CNTs (0.8688  $\mu\text{g}/\text{mL}$ ) was more potent than that of free doxorubicin (2.117  $\mu\text{g}/\text{mL}$ ). The mechanism of cell death predominantly involves early and late apoptosis.<sup>29</sup> Additionally, MWCNTs functionalized with a fluorochrome, radionuclide and folic acid and loaded with methotrexate had particle sizes of  $413.1 \pm 10.3$  nm, lengths of 400 to 700 nm and diameters of 20 to 60 nm. The release of methotrexate after 48 h in the rat plasma was 25 to 28%, while it was approximately 66% for the A549 cell extract. The stability of drug-loaded CNTs was more than 90% after 24 h in PBS, whereas it was approximately 85% in vivo. The drug-conjugate was taken up by A549 cells via folate receptor-dependent endocytosis, and 50% cell death was observed at 2.13  $\mu\text{g}/\text{ml}$ .<sup>30</sup>

In another report, polyethylene glycol-grafted oxidized MWCNTs were used to carry etoposide and Bcl-2 phosphorothioate antisense deoxyoligonucleotides (Aso) to exert cytotoxic effects on NCIH2135 NSCLC cells. Bcl-2 interference considerably improved the cytotoxic effects of etoposide on resistant NSCLC cells. The number of apoptotic cells increased significantly after treatment with CNTs. The release of etoposide and Aso increased considerably at pH 4.8 (88 and 31%) compared with pH 7.4 (44 and 22%). CNTs decreased the  $\text{IC}_{50}$  value toward the cancerous cells from  $41.0 \pm 3.8$   $\mu\text{M}$  for free etoposide to  $9.8 \pm 0.7$   $\mu\text{M}$  and caused a decline in Bcl-2 expression and an increase in intracellular ROS and apoptotic cell volume (24.5%).<sup>31</sup> Additionally, MWCNTs conjugated with dexamethasone and loaded with doxorubicin were less toxic to

red blood cells and more cytotoxic toward A549 cells compared with free doxorubicin and free MWCNTs. The sustained release of doxorubicin was observed at pH 5.5 until 200 h.<sup>32</sup> Oxidized MWCNTs with diameters of 50 to 80 nm and lengths of 10 to 20  $\mu\text{m}$  were functionalized with hyaluronic acid and conjugated with carboplatin to exert cytotoxic effects against TC-1 lung cancer cells. The internalization of CNTs conjugated with carboplatin into the cytoplasm of cancer cells was higher than that of unconjugated CNTs leading to a decline in metabolic activities. This effect was the result of an increase in ROS production leading to selective hyaluronic acid-receptor-mediated endocytosis.<sup>33</sup>

In an interesting study, cisplatin-loaded MWCNTs (~5 to 15 nm) sensitized cisplatin-resistant A549/DDP cells to cisplatin therapy. The analysis of the cytotoxic effects of MWCNTs without the drug indicated that the antiproliferative effects were due to cisplatin loaded onto the MWCNTs and not due to the CNTs. The uptake of CNTs into the cytoplasm of cancer cells was duration dependent. The probable mechanism of cell death induced by the cisplatin-loaded CNTs was dependent on apoptosis via the upregulation of Bax, Bim, Bid and caspases 3 and 9. In addition, the MWCNTs caused the downregulation of mesenchymal markers such as vimentin and N-cadherin (N-cad) along with EMT-induced transcription factors such as Snail, Slug and Twist1 leading to the reversal of cisplatin resistance.<sup>34</sup> The cytotoxic effects of MWCNTs on NSCLC cells in vitro are presented in Table 1.

**Table 1** Cytotoxic Effects of MWCNTs on NSCLC Cells in vitro

S. No	Drug Loaded on MWCNTs	Particle Dimensions	Cell Line, Cytotoxic Dose ( $\text{IC}_{50}$ )	Effects or Outcomes	Ref.
1.	Bromocriptine	Diameter of 25 to 40 nm, lengths ~ 500 nm	A549, 49.20 $\mu\text{g}/\text{mL}$	Upregulation of dopamine receptors DRD2 and DRD4, pro-apoptotic Bax and downregulation of anti-apoptotic Bcl-2	[25]
2.	Naringenin	Diameter of $9.6 \pm 1.4$ nm	A549, $82.6 \pm 7.3$ $\mu\text{g}/\text{mL}$	-	[26]
3.	Bcl-2 inhibitor ABT737	250 to 400 nm long	A549	Inhibition of Bcl-2, promotion of Bax, elevated ROS, cytochrome C release and resultant apoptosis	[27]
4.	Docetaxel	40–50 nm in length and 150–200 nm wide	A549, $0.32 \pm 0.01$ $\mu\text{g}/\text{mL}$	Apoptosis, sub-G1 phase arrest	[28]
5.	Doxorubicin	Lengths of 1 to 2 $\mu\text{m}$ and diameters of 20 to 30 nm	A549, 0.8688 $\mu\text{g}/\text{mL}$	Involvement of early and late apoptosis	[29]
6.	Methotrexate	Lengths of 400 to 700 nm and diameters of 20 to 60 nm	A549, 2.13 $\mu\text{g}/\text{mL}$	-	[30]
7.	Etoposide and Bcl-2 phosphorothioate antisense deoxyoligonucleotides	-	NCIH2135, $9.8 \pm 0.7$ $\mu\text{M}$	Bcl-2 interference, increase in intracellular ROS and apoptosis	[31]
8.	Carboplatin	Diameters of 50 to 80 nm and lengths of 10 to 20 $\mu\text{m}$	TC-1	Loss of mitochondrial and metabolic activities along with increased ROS production	[33]
9.	Cisplatin	~5–15 nm	A549/DDP	Involvement of apoptosis via the upregulation of Bax, Bim, Bid, Caspases 3 and 9 along with downregulation of vimentin and N-cad, Snail, Slug and Twist1	[34]

## Cytotoxic Effects of SWCNTs

SWCNTs functionalized using sodium alginate and chitosan with diameters ranging from 48 to 50 nm possessed prominent loading efficiency for curcumin (91%). The release of curcumin was continuous and augmented from physiological pH 7.4 (28.6%) to lysosomal pH 5.5 (91.2%) over a period of 72 h. The cytotoxic effects were prominent in A549 cells (36% viability) compared with NIH 3T3 fibroblasts (75% viability) after treatment with CNTs at a dose of 12  $\mu\text{g}/\text{mL}$ . The increase in dosage of CNTs from 4  $\mu\text{g}/\text{mL}$  (greater percentage of early apoptotic cells) to 20  $\mu\text{g}/\text{mL}$  resulted in a higher percentage of late apoptotic cells.<sup>35</sup> Similar to this report, carboxylated SWCNTs with diameters of less than 30 nm increased in size after being loaded with paclitaxel. The CNTs were efficacious in loading (120%), embedding (80%) and the release of paclitaxel (less than 50% after 12 h at pH 7.4). At a pH of 5.5, the rate of release surpassed 60%. The viability percentage of fibroblasts was higher (80%) than that of the A549 cells (70%) at the dose of 80  $\mu\text{g}/\text{mL}$ . Cell death was linked to an increase in intracellular ROS and damage to cell membranes, which was associated with the induction of apoptosis (elevated caspase-3 and activated PARP) via enhanced activation of MAPK.<sup>36</sup> In a similar study, the cytotoxic effects of SWCNTs synergized with paclitaxel with average diameters of  $\sim 0.8$  to 1 nm were tested on A549 and NCI-H460 cells. The outcomes indicate that the cytotoxic effects of SWCNTs were due to the increase in intracellular ROS (300%), the resultant activation of MAPK and the induction of apoptosis.<sup>37</sup> SWCNTs synthesized using different catalysts with a diameter range of 0.88 to 1.42 nm and lengths of 1 to 10  $\mu\text{m}$  were tested against A549 cells in this study. In accordance with the study, the SWCNTs were internalized effectively leading to a decrease in the glutathione, ATP content and metabolic rates of the carcinoma cells.<sup>38</sup>

In the same manner, SWCNTs (lengths of 1 to 50  $\mu\text{m}$  and diameters of less than 2 nm) functionalized with polyethylenimine and betaine were used for codelivery of survivin siRNA and doxorubicin into A549 cells. The drug-loading efficiency of the SWCNTs was more than 90%, and the rate of release of doxorubicin was comparatively higher at pH 5.0 (30%) to pH 7.4 (15%) after 72 h, with better cellular internalization via endocytosis. The  $\text{IC}_{50}$  for the toxic effects of CNTs on A549 cells was 63.46  $\mu\text{g}/\text{mL}$ .<sup>39</sup> Additionally, PEGylated SWCNTs with diameters of 50 nm loaded with gemcitabine released the drug at a faster rate at pH 5.0 than at pH 7.4. The drug loading efficiency of the CNTs was  $44.86 \pm 2.30\%$  and 50% cell death of A549 cells was observed at a dose of 12.79 nM. The higher uptake of the drug was due to endocytosis-mediated cellular internalization.<sup>40</sup> Interestingly, SWCNTs embedded with tumor-necrosis factor related apoptosis-inducing ligand (diameters of  $1 \pm 0.2$  nm, lengths of 100 to 100 nm) caused 50% cell death of H1703 cells by caspase-8 dependent apoptosis at a dose of 8 ng/mL. The cytotoxic effects of SWCNTs loaded with the drug were as effective as those of the free TRAIL.<sup>41</sup> Demonstrating a similar trend, SWCNTs functionalized with  $17\beta$ -estradiol and loaded with doxorubicin (diameters of 4 to 5 nm and lengths of 400 to 500 nm, 80% drug load) were stable for durations greater than 48 h and the  $\text{IC}_{50}$  for A549 cells was 11  $\mu\text{g}/\text{mL}$ .<sup>42</sup> The cytotoxic effects of SWCNTs on NSCLC cells in vitro are presented in Table 2.

## Antitumor Effects of Drug-Loaded CNTs on NSCLC Cells in vivo

MWCNTs with diameters of 20 to 30 nm, lengths of 0.5 to 2  $\mu\text{m}$  and incorporated with immunoadjuvants (cytosine–phosphate–guanine oligodeoxynucleotide and anti-CD40 Ig) aided the presentation of ovalbumin in a C57BL/6 pseudo–metastatic (B16F10) lung cancer model with no signs of multiorgan toxicity. The growth of OVA–expressing B16F10 melanoma cells was significantly inhibited after delivery of the antigenic ovalbumin using MWCNTs incorporated with immunoadjuvants.<sup>43</sup> Functionalized MWCNTs with an average size of 20 to 30 nm were used to deliver siRNA (siPLK1) into the intratumoral region of Calu6 tumors (4  $\mu\text{g}$  per tumor) specifically for targeting PLK1. The administration of CNTs promoted a substantial decline in PLK1 mRNA ( $67\% \pm 6\%$ ) and protein levels ( $38\% \pm 8\%$ ). There was a decrease in tumor volume, an increase in therapeutic quadrupling durations and survival of female Swiss nude mice after the administration of MWCNTs into the tumors. The MWCNTs were tumor-bound and led to a higher retention of siRNA in the tumor. The materials were not detected in major organs, which seems to be indicative of their limited toxicity and elevated targeting index. Tumor cell death was mediated by the induction of apoptosis and necrosis.<sup>44</sup> Identical results were reported by another group engaging the same type of CNTs, siRNA and dose into a female CD1 nude mouse model. A significant reduction in tumor growth and volume along with enhanced survival of tumor-induced mice was observed. The tumor-inhibitory effects were mediated by apoptosis and necrosis.<sup>45</sup>

**Table 2** Cytotoxic Effects of SWCNTs on NSCLC Cells in vitro

S. No	Drug Loaded on SWCNTs	Particle Dimensions	Cell Line, Cytotoxic Dose (IC <sub>50</sub> )	Effects or Outcomes	Ref.
1.	Curcumin	Diameters of 48 to 50 nm	A549, 12 µg/mL (36% viability)	Increase in percentage of early and late apoptosis	[35]
2.	Paclitaxel	Diameters <30 nm	A549, 70% viability at 80 µg/mL	Increase in intracellular ROS, damage to cell membranes, induction of apoptosis by elevated caspase-3, activated PARP and enhanced activation of MAPK	[36]
3.	Paclitaxel	Diameters of ~ 0.8 to 1 nm	A549 and NCI-H460	Increase in intracellular ROS, activation of MAPK and the induction of apoptosis	[37]
4.	Nickel, yttrium and iron catalysts	Diameters of 0.88 to 1.42 nm and lengths of 1 to 10 µm	A549	Decrease in the glutathione, ATP content and metabolic rates	[38]
5.	Survivin siRNA and doxorubicin	Lengths of 1 to 50 µm and diameters of < 2 nm	A549, 63.46 µg/mL	–	[39]
6.	Gemcitabine	Diameters of 50 nm	A549, 12.79 nM	–	[40]
7.	TRAIL	Diameters of 1 ± 0.2 nm, lengths of 100 to 1000 nm	H1703, 8 ng/mL	Caspase-8 dependent apoptosis	[41]
8.	Doxorubicin	Diameters of 4 to 5 nm, lengths of 400 to 500 nm	A549, 11 µg/mL	–	[42]

Female BALB/c mice injected subcutaneously with the 4T1 breast cancer cell line displayed metastasized tumors of the lung. The subcutaneous administration (0.1 mg per mouse) of oxidized MWCNTs with a mean length of 974 nm resulted in the recruitment of macrophages toward the site of administration. CNT-attracted macrophages were prohibited from entering the tumor microenvironment through such behavior. The CNTs accumulated more in the subcutaneous region, resulting in the reduction of macrophages and the vessel density compared with the control. Subsequently, the MWCNTs inhibited the tumor metastasis of 4T1 cells into the lung. This demonstrates that the MWCNTs possess antimetastatic properties with regard to tumors of the lung.<sup>46</sup>

SWCNTs intended to carry gemcitabine (25 mg/kg) into A549 tumor-induced B6 athymic nude mice induced a decrease in tumor size after 17 days, which was much better than the results in the drug-alone group, and the effects were not due to the CNTs. This decrease in tumor size continued to improve considerably after 23 days, and the extended duration of circulation of the drug in the blood was due to the enhanced permeability and retention effect (EPR effect). The survival of CNT-treated mice improved from approximately 50 days to three months compared with the control groups.<sup>40</sup> The antitumor effects of CNTs on NSCLC cells in vivo are listed in Table 3. The uptake and cellular fate of CNTs loaded with anticancer molecules are presented in Figure 1.

## Rationale for the Cytotoxic Effects of CNTs on Cancer Cells

### MWCNTs Induce Cytoskeletal Incompetence Due to Their Intrinsic Antitumor Properties

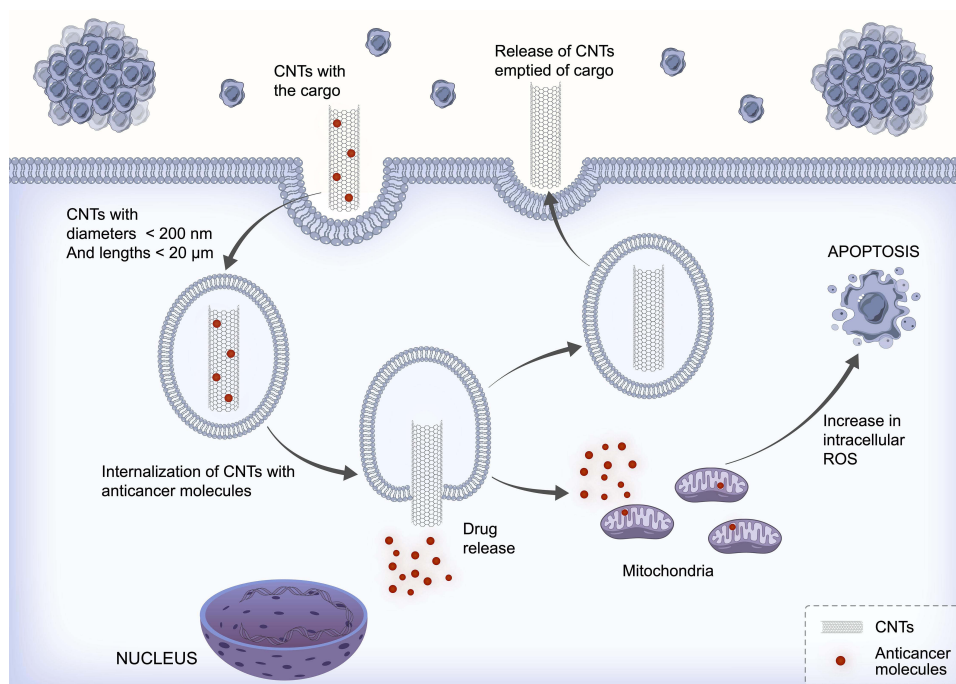
MWCNTs resemble microtubules in several ways that include the shape, length, resilient properties of strength and elasticity along with their reactive surfaces. Based on this resemblance, CNTs can cause instability of the cytoskeletal system, specifically the centrosome, leading to disruption of microtubule organization. This can affect the migrating and

**Table 3** Antitumor Effects of CNTs in vivo

S. No	Type of CNTs and Dimensions	Drug Load and Route of Administration	Animal Model	Effects or Outcomes	Ref.
1.	MWCNTs, diameters of 20 to 30 nm, 0.5 to 2 $\mu\text{m}$ length	Immunoadjuvants and antigenic ovalbumin	C57BL/6 mice	Inhibition of metastatic growth in lungs and improved survival of tumor mice	[43]
2.	MWCNTs, sizes of 20 to 30 nm	siPLK1, intratumoral region	Female Swiss nude mice	1. Decrease in tumor volume mediated by apoptosis and necrosis 2. Decline in PLK1 mRNA and protein levels	[44]
3.	MWCNTs, Diameters of 20–30 nm, and lengths of 0.5–2 $\mu\text{m}$	siPLK1, intratumoral administration	Female CD1 nude mice	1. Reduction in tumor growth and volume with enhanced survival 2. Apoptosis and necrosis of tumor cells	[45]
4.	MWCNTs, length of 974 nm	Subcutaneous administration	Female BALB/c mice	Reduction of macrophages, vessel density and inhibition of metastatic growth in lungs	[46]
5.	SWCNTs, diameters of 50 nm	Gemcitabine, Intravenous tail injection	B6 athymic nude mice	Decrease in tumor size and improved survival	[40]

proliferating properties of cells in vitro or in vivo. Individual CNTs can induce such effects as nanosized materials, whereas CNTs loaded onto a template do not interact with the cytoskeleton as they behave identically to submicrometric materials at similar doses. Hence, functionalized MWCNTs or MWCNTs attached to templates are not cytotoxic, but are effectively biocompatible compared with individual CNTs.<sup>47</sup>

For instance, CNTs with 3 to 12 walls and an external diameter range of 5 to 15 nm possessed significant antimigratory properties at a 50  $\mu\text{g/mL}$  dose and cytotoxic effects at a slightly higher dose of 75  $\mu\text{g/mL}$ . At higher doses, the MWCNTs bind to the protofilament surface of microtubules of the cancer cells to exert these cytotoxic effects.<sup>48</sup> By interfering with the dynamics of the microtubules, CNTs can lead to blockage of cell division and malsegregation of the chromosomes resulting in

**Figure 1** Schematic representation of the uptake and cellular fate of CNTs loaded with anticancer molecules.

an apoptotic trigger. This is demonstrative of the fact that individual MWCNTs interfere with microtubules to exert their cytotoxic effects. In this regard, MWCNTs enter the cancer cell cytoplasm and interact with the microtubules behaving as tubulin scaffolds. At this juncture, they can promote tubulin nucleation and microtubule assemblage, resulting in reduced microtubule dynamics and the formation of mitotic spindle aberrations. Hence, MWCNTs can by themselves act as therapeutic agents for cancer in nanomedicine due to their intrinsic anti-proliferative and anti-migratory properties.<sup>49</sup> Supporting this intrinsic anticancer property, A549 cells treated with MWCNTs (0.5–100  $\mu\text{g/ml}$ ) showed time- and dose-dependent cell death wherein the concentrations higher than 50  $\mu\text{g/ml}$  elicited elevated responses owing to oxidative stress and apoptosis.<sup>50</sup> In vivo, MWCNTs possessed significant antitumor properties as evidenced by reduced tumor progression and growth of malignant and drug-resistant tumors.<sup>51</sup>

Therefore, MWCNTs are biomimetic due to their resemblance of microtubules and they can possibly induce changes in protofilaments causing the microtubules to fail in their ability to depolymerize significantly. This can result in reduced ability of the cells to migrate. In addition, MWCNTs can induce the formation of abnormal spindles and lead to mitotic blockage and proapoptotic effects in actively proliferating cells, whereas, in cancer cells that are resistant, they can stimulate aneuploidy and behave as clastogens. Relating more to this behavior, CNTs must be dispersed in the absence of a template for interacting with tubulins in the process of eliciting a biological response. Additionally, MWCNTs can be loaded with anticancer drugs by  $\pi$ - $\pi$  stacking which can enhance the effects of these drugs known to interfere with microtubules. This synergism can promote the antitumor effects of standard drugs and inhibit resistance among cancer cells.<sup>52</sup>

## SWCNTs Interact with Nucleic Acids for Their Cytotoxic Effects

As discussed above, MWCNTs interact with microtubules due to their size, whereas SWCNTs interact and adsorb with nucleic acids, especially DNA due to their diameter. This can help improve the purification and solubility of SWCNTs.<sup>53,54</sup> This may also assist SWCNTs in their biomedical use as they can transport loads of DNA or other nucleic acids and protect them from cellular digestion by a variety of cells in animal models.<sup>55</sup> Additionally, SWCNTs functionalized with lysine or ammonium and complexed with plasmid DNA exhibited higher gene transfer abilities and enhanced expression (up to 10-fold) than the free DNA forms.<sup>56,57</sup> Similarly, siRNA conjugated with SWCNTs efficiently silenced the targeted genes and inhibited the growth of lung tumors in vivo.<sup>58,59</sup> Likewise, high-molecular-weight anticancer proteins that cannot enter cancer cells have been internalized by conjugation with SWCNTs.<sup>60</sup> Therefore, SWCNTs bind strongly to biological macromolecules such as DNA, RNA and proteins, which may possess important cellular functions. This can interrupt critical cellular functions, leading to oxidative stress and simultaneous cytotoxic effects.<sup>61</sup>

In this regard, SWCNTs can enter the lipid bilayer of cancer cells and gather inside the nucleus. Later, they can bind to the major grooves of DNA and stabilize the i-motif DNA of the telomeres. This results in the inhibition of telomerase activity and irregular functioning of the telomeres, which can lead to DNA damage, upregulated expression of tumor suppressors and inhibition of neoplastic growth by cell cycle arrest, apoptosis and senescence.<sup>62,63</sup>

## Toxic Effects of CNTs at the Preclinical Level

### Toxicity of CNTs in vitro on Normal Lung Cells

MWCNTs with average lengths of 3.86  $\mu\text{m}$  and diameters of  $49 \pm 13.4$  nm were exposed (1.2  $\mu\text{g/ml}$ ) to an in vitro model containing cocultured SAEC and HMVECs mimicking alveolar-capillary interactions. The exposure of MWCNTs to epithelial model SAECs resulted in changes in the endothelial HMVEC barrier model. There was an increase in ROS levels, angiogenesis and gap formation concomitant with the loss of VE-cadherin and other changes in the organisation of actin. The secretion of inflammatory mediators, such as vascular endothelial growth factor A (VEGFA), soluble intracellular adhesion molecule 1 (sICAM-1) and soluble vascular cell adhesion molecule 1 (sVCAM-1), was amplified along with an increase in intracellular phospho-NF- $\kappa$ B, phospho-Stat3, and phospho-p38 MAPK.<sup>64</sup>

Likewise, BEAS-2B cells exposed to MWCNTs with average lengths of 1.12  $\mu\text{m}$  and diameters of 65 to 70 nm at a sublethal concentration of 44  $\mu\text{g/ml}$  for 96 h lost their organized epithelial structure. Additionally, the expression levels of E-cadherin (E-cad) and  $\beta$ -catenin were decreased parallel to the increased expressions of vimentin and  $\alpha$ -SMA. The expression levels of ECM-linked fibronectin and MMPs such as MMP-2 and MMP-9 were also elevated. The promotion

of EMT as a result of a decrease in E-cad was linked to the accumulation of SNAIL-1 in the nucleus, phosphorylation of GSK-3 $\beta$  in the cytosol, participation of phosphorylated Akt and a resultant increase in production of TGF- $\beta$ .<sup>65</sup> Related to this report, the expression of markers related to the transition of fibroblasts to become myofibroblasts, such as FSP-1,  $\alpha$ -SMA, and collagen III, was elevated in NIH 3T3 cells after exposure to MWCNTs (20 to 50  $\mu$ m, 30  $\mu$ g/mL). Moreover, the expression of E-cad diminished, whereas, the expression of fibronectin was enhanced.<sup>66,67</sup> The differential expression of these ECM-related proteins after contact with MWCNTs could be considered determinants or possible markers for EMT induced by the exposure considered to be toxic to normal lung cells.

## Toxicity of CNTs in vivo

### Pulmonary Toxicity of CNTs

The pharyngeal aspiration of MWCNTs into C57BL/6 mice caused a decline in E-cad levels and an elevation in vimentin levels. As a consequence of exposure to CNTs, the mice developed lung fibrosis.<sup>65</sup> Similarly, MWCNTs induced EMT and fibrosis specifically, specifically in E-cad-positive fibroblasts and epithelial cells in lung tissues of hypertensive rats by activating the TGF- $\beta$ /Smad2 pathway. Long MWCNTs (20 to 50  $\mu$ m) were more potent in promoting fibrosis, deposition of collagen and formation of granulomas in male spontaneously hypertensive rats (0.6 mg/rat) compared with their shorter counterparts (0.5 to 2  $\mu$ m).<sup>66,67</sup>

Similarly, MWCNTs were administered to female C57BL/6 mice through the oropharyngeal aspiration (10 or 40  $\mu$ g) or inhalation (aerosol mass of 6.2 to 8.2 mg/m<sup>3</sup>) routes for 4 days to mimic the exposure of toxic materials in a work environment. Inhalation exposure and 10  $\mu$ g aspiration resulted in enhanced infiltration of eosinophils into the lungs, increased mucus production with a lung burden of 600 to 800  $\mu$ g/m<sup>2</sup> alveolar epithelium and increased secretion of IL-13. A set of 154 differentially expressed genes were observed to be common between lungs exposed to MWCNTs via both routes.<sup>68</sup> In the same manner, the intratracheal administration of MWCNTs (5 to 50 mg/kg) led to neutrophilia, leading to inflammation of the lungs in ICR male mice. The expression of a set of proinflammatory cytokines (TNF- $\alpha$ , IFN- $\gamma$  and interleukins-1, 4, 5, 6, 10 and 12) was increased along with the volume of B cells and IgE.<sup>69</sup>

Two types of MWCNTs named MWCNT1 (lengths of 13  $\mu$ m and diameters of 40 to 100 nm) and MWCNT2 (lengths of 5  $\mu$ m and diameters of 30 nm) were used for determination of toxicity in female C57Bl6/J mice by pharyngeal aspiration of 1 mg/ml per 20 g body weight (40  $\mu$ l). The expression levels of the systemic inflammation marker monocyte chemoattractant protein-1 (MCP-1) and profibrotic markers such as matrix metalloproteinase-8 (MMP-8) and tissue inhibitor of metalloproteinase-1 (TIMP-1) were upregulated after exposure to MWCNT1. Although the formation of granulomas was observed after exposure to both types of CNTs, the changes in serum markers and hyperplasia were more prominent in MWCNT1-exposed mice.<sup>70</sup>

### Systemic Toxicity of CNTs

For analysis of the systemic toxicity of CNTs to multiple organ systems, female C57BL/6 mice exposed to SWCNTs (40–80  $\mu$ g/mouse) through single pharyngeal aspiration showed elevated levels of free radical adducts in lungs, heart and liver tissues. Increased recruitment of neutrophils, elevated levels of LDH and proinflammatory cytokines such as TNF- $\alpha$  and IL-6 were observed. Progressing toward granulomatous bronchointerstitial pneumonia, collagen deposition and pulmonary fibrosis (indicated by TGF $\beta$ 1 release) as the characteristics of lung inflammation arising as a consequence of lung injury caused by SWCNTs was increased. Alterations in the functioning of the lungs were also observed.<sup>71</sup> Male spontaneously hypertensive rats were exposed to SWCNTs (0.6 mg/rat) via nonsurgical intratracheal instillation for 2 days resulting in increases in the levels of myeloperoxidase as an indicator of lung injury and the volumes of inflammatory cells such as PMNs, macrophages and lymphocytes. Substantial increases in LDH, total protein and albumin levels were detected, accompanied by increased proinflammatory cytokines such as MIP-2, IL-6 and TNF- $\alpha$  and decreased anti-inflammatory CC16 levels. As an indicator of oxidative stress, HO-1 levels were increased along with liver function markers such as ALT, AST, creatine kinase and LDH. The marker for endothelial dysfunction endothelin-1 was increasingly expressed together with angiotensin-converting enzyme indicating cardiac injury and subsequent damage to the heart, brain and kidney. Histological studies also indicated damage to the lungs and heart of the exposed rats.<sup>72</sup>

Similarly, SWCNTs with diameters of 1.2 to 1.5 nm and lengths of 2 to 5  $\mu\text{m}$  were administered to male and female MITO-Luc and CD1 mice at doses of 0.16, 1.6 and 6.4 mg/kg with the intentions of acute and chronic (up to nine weeks) exposure through the tail vein. The administration of SWCNTs resulted in a systemic increase in the proliferation of immune cells and mobilizing ability inside the bone marrow of MITO-Luc mice. Administering SWCNTs to CD1 mice at acute and chronic levels caused an increase in the ingestion of water and food. Chronic exposure led to symptoms linked to cholestasis and elevation of liver parameters. Although the lungs and livers had higher accumulations of SWCNTs, the liver was the dominant site of accumulation. Increases in CD45<sup>+</sup> and CD68<sup>+</sup> cells indicated inflammation of the hepatocytes involving the M1 macrophages. These effects subsided or returned to near-normalcy after 3 weeks of withdrawal of administration.<sup>73</sup> The local and systemic toxic effects of CNTs are provided in Table 4 and Figure 2.

**Table 4** Local and Systemic Toxicity of CNTs in vitro and in vivo

S. No	Type of CNTs, Dimensions and Dose	Route of Administration	Cell Line or Animal Model	Effects or Outcomes	Ref.
1.	MWCNTs, lengths of 3.86 $\mu\text{m}$ and diameters of 49 $\pm$ 13.4 nm, 1.2 $\mu\text{g}/\text{mL}$	–	Co-cultured SAEC and HMVECs	1. Increase in ROS levels, angiogenesis and loss in actin arrangement 2. Increase in inflammatory mediators such as VEGFA, sICAM-1, sVCAM-1 and phospho-NF- $\kappa$ B, phospho-Stat3, and phospho-p38 MAPK	[64]
2.	MWCNTs, lengths of 1.12 $\mu\text{m}$ and diameters of 65 to 70 nm	Pharyngeal aspiration	44 $\mu\text{g}/\text{mL}$ in vitro BEAS-2B cells and 50 $\mu\text{L}$ in vivo in C57BL/6 mice	1. Decreased expressions of E-cad and $\beta$ -catenin and increased expressions vimentin and $\alpha$ -SMA, MMP-2, MMP-9 and TGF- $\beta$ (in vitro) 2. Lung fibrosis elicited by a decline in E-cad levels and an elevation in vimentin levels (in vivo)	[65]
3.	MWCNTs, 20 to 50 $\mu\text{m}$	Non-surgical intratracheal instillation	30 $\mu\text{g}/\text{mL}$ in vitro NIH 3T3 cells, 0.6 mg/hypertensive rat in vivo	1. Elevation of FSP-1, $\alpha$ -SMA, collagen III and fibronectin levels, diminished E-cad levels. Engagement of the TGF- $\beta$ /Smad2 pathway (in vitro) 2. Fibrosis, deposition of collagen and formation of granuloma in vivo	[66,67]
4.	MWCNTs, lengths of 5 to 13 $\mu\text{m}$ and diameters of 30 to 100 nm	Pharyngeal aspiration	1 mg/mL per 20 gm body weight of female C57Bl6/J mice	Upregulated expressions of MCP-1, MMP-8 and TIMP-1, changes in serum markers, hyperplasia and formation of granulomas	[70]
5.	SWCNTs, 40–80 $\mu\text{g}/\text{mouse}$	Pharyngeal aspiration	Female C57BL/6 mice	1. Increased recruitment of neutrophils, elevated levels of LDH and pro-inflammatory cytokines such as TNF- $\alpha$ and IL-6 2. Granulomatous bronchointerstitial pneumonia, collagen deposition and pulmonary fibrosis	[71]

(Continued)

Table 4 (Continued).

S. No	Type of CNTs, Dimensions and Dose	Route of Administration	Cell Line or Animal Model	Effects or Outcomes	Ref.
6.	SWCNTs, 0.6 mg/rat	Non-surgical intratracheal instillation	Male spontaneously hypertensive rats	<ol style="list-style-type: none"> <li>Increases in myeloperoxidase and the volumes of inflammatory cells such as PMNs, macrophages and lymphocytes.</li> <li>Elevation in pro-inflammatory cytokines such as MIP-2, IL-6 and TNF-<math>\alpha</math> and decrease in anti-inflammatory CCL6 levels</li> <li>Changes in oxidative stress and liver function markers</li> <li>Increases in Endothelin-1 and angiotensin-converting enzyme indicating cardiac injury and subsequent damages to heart, brain and kidney</li> </ol>	[72]
7.	SWCNTs, diameters of 1.2 to 1.5 nm and lengths of 2 to 5 $\mu$ m, 0.16, 1.6 and 6.4 mg/kg	Intravenously into tail vein	MITO-Luc and CDI mice	<ol style="list-style-type: none"> <li>Cholestasis and elevation of liver parameters</li> <li>Increases in CD45+ and CD68+ cells</li> </ol>	[73]

## Genotoxicity and Oncogenic Potential of CNTs without Drug Conjugates Toxic Potential of MWCNTs

After exposure of MWCNTs (with sizes of  $\sim$ 1100 nm) to GDL1 *gpt* delta mouse lung fibroblasts cocultured with RAW264.7 cells at 20 and 80  $\mu$ g/mL, a concentration-dependent uptake of CNTs was observed. The *gpt* mutant frequencies (MTs) were augmented in the cocultured cells, whereas increased ROS production and elevated IL-1 $\beta$  and TNF- $\alpha$  levels were observed in RAW264.7 cells after exposure to CNTs. In addition, 8-oxo-dG levels representing the formation of DNA adducts were elevated

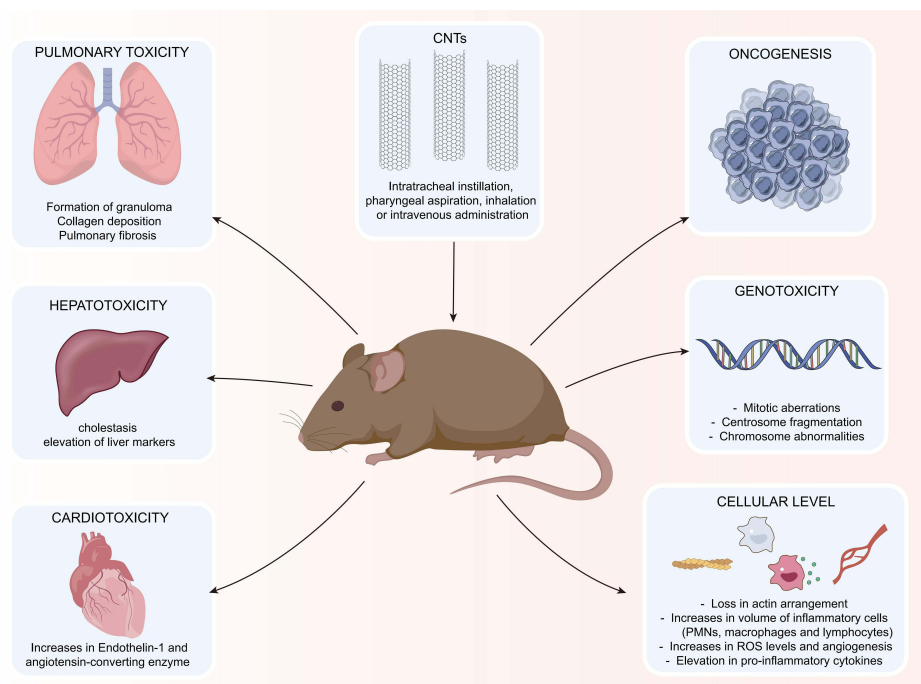


Figure 2 Illustration of the systemic toxicity of CNTs in animal models.

in GDL1 cells.<sup>74</sup> Multiple types of MWCNTs with average diameters of 30 to 57 nm and lengths of 2 to 5  $\mu\text{m}$  at doses of 0.024 and 24  $\mu\text{g}/\text{mL}$  exhibited cytotoxicity in BEAS-2B cells, leading to mitotic aberrations, centrosome fragmentation and chromosome abnormalities engaging in cell cycle arrest (predominantly at the G1 and G2 phases) with increased clonal growth.<sup>75</sup> Additionally, SAEC and HMVEC lung microvascular cells were cocultured and exposed to MWCNTs (lengths of 3.86  $\mu\text{m}$  and width of  $49 \pm 13.4$  nm) at a dose of 1.2  $\mu\text{g}/\text{mL}$  or 0.25  $\mu\text{g}/\text{cm}^2$  in vitro. In vivo, male C57BL/6J mice were exposed to 10, 20, 40, or 80  $\mu\text{g}$  of suspensions containing MWCNTs by pharyngeal aspiration. The outcomes indicated that a set of concordant genes and signaling pathways related to lung inflammation and fibrosis were actively involved in responses anticipated for MWCNTs. Such networks associated with inflammation, cellular repair, communication of immune cells, formation of blood cells and LXR/RXR activation of these concordant genes were significantly altered after exposure to MWCNTs.<sup>76</sup> Additionally, the intratracheal administration of MWCNTs (11.3 nm in diameter and 0.7  $\mu\text{m}$  in length) at 2 mg/rat promoted the formation of micronucleated pneumocytes via clastogenic and aneugenic behavior.<sup>77</sup>

In vitro, pSAECs exposed (0.06  $\mu\text{g}/\text{cm}^2$ ) to different types of laboratory-aged MWCNTs (1 to 12  $\mu\text{m}$  long, 13 to 18 nm wide) acquired neoplastic behavior with improved invasive and migratory properties. This transformation to the cancerous form was evident in epithelial cells exposed to every type of MWCNT. However, the MWCNTs that remained unfunctionalized led to the transformation of these cells to cancerous forms at the earliest duration compared with the other functionalized forms.<sup>78</sup> Similarly, the tail moment of lung DNA from male ICR mice at a dose of 0.2 mg/mouse was increased by intratracheal administration of CNTs. The body weights of guanine phosphoribosyltransferase (gpt) delta mice decreased after treatment with MWCNTs (70–110 nm in size, 2  $\mu\text{m}$  long, 0.2 mg/mouse). Considerable changes were observed in lung tissues as evidenced by histopathology. Macrophage and lymphocyte infiltration around alveoli and bronchi leading to hypergenesis were evident. The increase in instillations of MWCNTs to mice caused an upsurge in mutant frequencies. Immunohistochemistry showed intense patterns for oncogenic factors such as inducible nitric oxide synthase and nitrotyrosine. The occurrence of DNA adducts associated with oxidative stress and lipid peroxidation (8-oxodG, HedA, HedC, HedG) continued to increase in lung DNA until 72 h after exposure.<sup>79</sup>

Of the thirty rats administered with MWCNTs (diameter,  $76.49 \pm 31.14$  nm; length,  $8.79 \pm 4.41$   $\mu\text{m}$ ; 0.5 mg) by intratracheal-intrapulmonary spraying, sixteen rats died of malignant mesothelioma between 52 and 91 weeks. Macroscopic observations indicated color change of parabranchial and mediastinal lymph nodes to black after treatment with CNTs. Pulmonary collagen, as an oncogenic marker, and the PCNA index, as a marker for proliferation of cancer cells, were increased in the alveoli of MWCNTs-treated rats compared with control rats. The levels of chemotactic proteins, such as CCL2 and CCL3, were also elevated. Interestingly, CNTs were detected in the lungs from the onset of the experiment through sacrifice.<sup>80</sup> Identical to the previous report, administration of WHO MWCNTs (lengths of 5  $\mu\text{m}$  and diameters of 3  $\mu\text{m}$ ) at  $1 \times 10^9$  or  $5 \times 10^9$  counts into male Wistar rats through the intraperitoneal route induced malignant mesotheliomas in those animals. Mortality was significant in all treated groups until the end of the experiment at 24 months. Necropsy revealed blood-fluid rich ascites in the CNT-treated groups. Tumor nodules were predominantly observed in the diaphragm, liver and pancreas. The study stated that the ratio of lengths and diameters along with curvature determined the toxicity of the MWCNTs.<sup>81</sup>

## Toxic Potential of SWCNTs

Similarly, the exposure of human primary small airway epithelial cells (pSAECs) and BEAS-2B cells to 0.024  $\mu\text{g}$  SWCNT/ $\text{cm}^2$  led to the formation of multipolar mitotic spindles (characteristic of cancerous cells) with multiple centrosome fragments. The SWCNTs (diameter of 1 to 4 nm and lengths of 0.5 to 1  $\mu\text{m}$ ) were found to be associated with microtubules, DNA and the fragments of centrosomes. The behaviour of the SWCNTs presumes a substantial resemblance to clastogens and aneugens.<sup>82</sup> It is interesting to note that SWCNTs promote the B-DNA to A-DNA transition and preferentially bind to the GC content of the DNA major groove.<sup>83</sup> In addition, unfunctionalized SWCNTs (diameters of 20–40 nm and lengths of 1–5  $\mu\text{m}$ ) induced the formation of micronuclei and reduced the proliferation potential of lymphocytes at doses  $\geq 25$   $\mu\text{L}/\text{mL}$ . Remarkably, amide-functionalized SWCNTs induced micronuclei formation, but did not interfere with the proliferation potential. Likewise, at the same dose, the unfunctionalized SWCNTs induced DNA damage related to the  $\gamma$  H2AX foci (2.7-fold) of the fibroblasts, whereas, the damage caused by the functionalized SWCNTs was 3.18-fold greater. The MWCNTs used in the study behaved concurrently as clastogens and aneugens, much like the SWCNTs. This genotoxic behavior of SWCNTs could be attributed to their electrochemical properties.<sup>84</sup>

Summarizing the results of this section, the genotoxic and oncogenic potentials of CNTs without drug conjugates are presented in Table 5.

## Biomarkers of CNT-Mediated Oncogenesis and Toxic Effects

### Markers of SWCNT-Induced Toxicity

To study the markers for the oncogenic potential of CNTs, SWCNTs (0.1 to 1  $\mu\text{m}$  length and width of 0.8–1.2 nm) were treated against BEAS-2B cells (0.02  $\mu\text{g}/\text{cm}^2$  or 0.1  $\mu\text{g}/\text{mL}$ ) for 6 months. The cells in vitro possessed enhanced colony-forming

**Table 5** Genotoxicity and Oncogenic Potential of CNTs without Drug Conjugates

S. No	Type of CNTs and Dimensions	Animal Model or Cell Line	Dose and Route of Administration	Effects or Outcomes	Ref.
1.	MWCNTs, sizes of ~1100 nm	GDLI gpt delta mice lung fibroblasts co-cultured with RAW264.7	20 and 80 $\mu\text{g}/\text{mL}$	Increased ROS production and elevated IL-1 $\beta$ and TNF- $\alpha$ levels	[74]
2.	MWCNTs, diameters of 30 to 57 nm and lengths of 2 to 5 $\mu\text{m}$	BEAS-2B cells	0.024 and 24 $\mu\text{g}/\text{mL}$	Mitotic aberrations, centrosome fragmentation and chromosome abnormalities	[75]
3.	MWCNTs, lengths of 3.86 $\mu\text{m}$ and width of 49 $\pm$ 13.4 nm	SAEC and HMVEC lung microvascular cells (in vitro), male C57BL/6J mice (in vivo)	1.2 $\mu\text{g}/\text{mL}$ (in vitro), 10, 20, 40, or 80 $\mu\text{g}$ , pharyngeal aspiration (in vivo)	Occurrence of a set of concordant genes and signalling pathways related to lung inflammation and fibrosis	[76]
4.	MWCNTs, 11.3 nm in diameter and 0.7 $\mu\text{m}$ in length	Female Wistar rats	2 mg/rat, intratracheal	Formation of micronucleated pneumocytes	[77]
5.	Laboratory-aged MWCNTs, 1 to 12 $\mu\text{m}$ long, 13 to 18 nm wide	pSAECs	0.06 $\mu\text{g}/\text{cm}^2$	Cells developed neoplastic behaviour with improved invasive and migratory properties	[78]
6.	MWCNTs, 70–110 nm in size, 2 $\mu\text{m}$ long	Male ICR mice	0.2 mg/mice, intratracheal	1. Decrease in body weight, Macrophage and lymphocyte infiltration around alveoli and bronchi, 2. Upsurge in mutant frequencies and oncogenic factors 3. Occurrence of DNA adducts	[79]
7.	MWCNTs, 11.3 nm in diameter and 0.7 $\mu\text{m}$ in length	Female Wistar rats	2 mg/rat, intratracheal	Formation of micronucleated pneumocytes	
8.	MWCNTs, diameters of 76.49 $\pm$ 31.14 nm, lengths of 8.79 $\pm$ 4.41 $\mu\text{m}$	Rats	0.5 mg/ rat, intratracheal-intrapulmonary spraying	Increases in pulmonary collagen, PCNA index and chemotactic proteins such as CCL2 and CCL3	[80]
9.	MWCNTs, lengths of 5 $\mu\text{m}$ and diameters of 3 $\mu\text{m}$	Male Wistar rats	1 $\times$ 10 <sup>9</sup> or 5 $\times$ 10 <sup>9</sup> , intraperitoneal	Significant mortality, blood-fluid rich ascites and tumor nodules in diaphragm, liver and pancreas	[81]
10.	SWCNTs, diameter of 1 to 4 nm and lengths of 0.5 to 1 $\mu\text{m}$	Human primary small airway epithelial cells (pSAECs) and BEAS-2B cells	0.024 $\mu\text{g}$ SWCNT/ $\text{cm}^2$	Formation of multipolar mitotic spindles	[82]
11.	SWCNTs, diameters of 20–40 nm, and lengths of 1–5 $\mu\text{m}$	Human lymphocytes	25 $\mu\text{L}/\text{mL}$	Formation of micronuclei	[84]

abilities after being treated with CNTs. SOX9 expression was increased in CNT-treated cells by up to 15-fold compared with untreated cells. There was an increase in the expression of CD133, Nanog, SOX2 and Oct4. After administering the cells treated with CNTs intravenously at 10 µg/mouse lung (0.5 mg/kg body weight) to NOD/SCID gamma mice *in vivo*, the cancer cells found in the lungs showed elevated expression of SOX9, controlling the cancer stem-like cells by ALDH1A1.<sup>85</sup> Similar to this report, SWCNTs with the same physicochemical properties as mentioned above were treated against BEAS-2B cells (0.02 µg/cm<sup>2</sup>). The CNT-treated cells possessed downregulated expression of epithelial markers such as ZO-1, E-Cad, and Claudin-1, and upregulated expression of N-cad. Knockdown of the EMT regulator Slug in BEAS-2B cells upregulated the expression of E-cad and claudin-1 and downregulated the expression of N-cad. This demonstrates the role of Slug in EMT activation and transformation into an aggressive malignant phenotype of CNT-treated cells *in vitro*. *In vivo*, Slug was found to positively regulate oncogenesis and metastasis of NSG mice subcutaneously injected with CNT-treated cells.<sup>86</sup> Similar to the physicochemical properties and dosage of treatment, chronic exposure to SWCNTs enhanced the transformation toward malignancy of SAECs and BEAS-2B cells by acquiring cancer stem-like properties. These highly invasive phenotypes were resistant to apoptosis in a p53-dependent manner and were similar in properties to those of H460 lung cancer cells. These cells were injected into NSG immunodeficient mice, which gave rise to the formation of tumors. Mechanistically, the expression levels of Nanog, SOX2 and SOX17 were upregulated, while E-cad expression was decreased. CD24<sup>low</sup> and CD133<sup>high</sup> stem cell markers could be used as potential markers for SWCNT-mediated carcinogenesis.<sup>87</sup>

SWCNTs with diameters of 2 nm and lengths of 5 to 30 µm exhibited limited cytotoxic effects on BEAS-2B cells at a sublethal concentration of 10 µg/mL for a period of 60 days. The intracellular ROS levels increased with a significant loss in MMP and enhanced apoptosis compared with the controls *in vitro*. The SWCNT-exposed cells possessed improved migratory, invasive and colony-forming abilities. *In vivo*, BALB/c immunodeficient nude mice subcutaneously injected with the exposed cells developed tumors, with elevated expression of Ki67 and TTF-1, which are specific for malignant lung adenocarcinoma. A set of differentially methylated genes was expressed along with the upregulated expression of DNA methylases such as DNMT3a and DNMT1.<sup>88</sup> The mechanisms of SWCNT-mediated oncogenesis are listed in Table 6.

**Table 6** Mechanisms of SWCNTs-Mediated Oncogenesis

S. No	Type of CNTs and Dimensions	Animal Model or Cell Line	Dose and Route of Administration	Effects or Outcomes	Ref.
1.	SWCNTs, 0.1 to 1 µm length and width of 0.8–1.2 nm	BEAS-2B cells ( <i>in vitro</i> ), NOD/SCID gamma mice ( <i>in vivo</i> )	0.02 µg/cm <sup>2</sup> or 0.1 µg/mL ( <i>in vitro</i> ), 0.5 mg/kg - intravenous	1. Increased expressions of SOX9, CD133, Nanog, SOX2 and Oct4 ( <i>in vitro</i> ) 2. Elevated expressions of SOX9 regulating cancer stem-like cells by ALDH1A1 ( <i>in vivo</i> )	[85]
2.	SWCNTs, 0.1 to 1 µm length and width of 0.8–1.2 nm	BEAS-2B cells ( <i>in vitro</i> ), NOD/SCID gamma mice ( <i>in vivo</i> )	0.02 µg/cm <sup>2</sup> ( <i>in vitro</i> ), 1 × 10 <sup>6</sup> CNTs-treated BEAS-2B cells, subcutaneous ( <i>in vivo</i> )	1. Downregulated expressions of ZO-1, E-cad, Claudin-1 and upregulated expressions of N-cad ( <i>in vitro</i> ) 2. Oncogenesis and metastasis ( <i>in vivo</i> )	[86]
3.	SWCNTs, 0.1 to 1 µm length and width of 0.8–1.2 nm	SAECs and BEAS-2B ( <i>in vitro</i> ), NOD/SCID gamma mice ( <i>in vivo</i> )	0.02 µg/cm <sup>2</sup> ( <i>in vitro</i> ), 0.5 mg/kg ( <i>in vivo</i> )	1. Changed to highly invasive phenotypes <i>in vitro</i> 2. Formation of tumors, upregulated Nanog, SOX2, SOX17 expressions and downregulated E-cad expressions ( <i>in vivo</i> )	[87]
4.	SWCNTs, diameters of 2 nm and lengths 5 to 30 µm	BEAS-2B cells ( <i>in vitro</i> ), BALB/c immunodeficient nude mice ( <i>in vivo</i> )	10 µg/mL <i>in vitro</i>	1. CNTs-exposed cells possessed improved migratory, invasive and colony-forming abilities. Increased intracellular ROS levels with a significant loss in MMP and enhanced apoptosis were observed after treatment <i>in vitro</i> . 2. Formation of tumors with elevated expressions of Ki67, TTF-1, DNA methylases and occurrence of differentially methylated genes <i>in vivo</i> .	[88]

## Markers of MWCNT-Induced Toxicity

In an interesting report, a list of potential biomarkers was identified as concordant between mouse tissue and blood with SAEC and HMVECs after treating male C57BL/J6 mice with MWCNTs ( $3.86 \pm 1.9 \mu\text{m}$  length and  $49 \pm 13.4 \text{ nm}$  width, mean). Among mouse tissues and SAECs, exposure to MWCNTs for one month resulted in downregulated mRNA expression of CAND1, CYCS, DENND5B, HS3ST3B1, MAML1, MAN2B2, METTL21, PIGS, PPP1C, SEL1L, SH3BP2, SLC7A1, TGM2, and XRN2 and upregulated expression of S100A5. After exposure for six months, KIF14 and TLL7 expression was downregulated, whereas the expression of MYBPC2 and PSD4 was upregulated. Twelve months post-exposure, ADH5, ANLN, ARF1, CCDC115, CYCS, DDX24, FAM188A, IKZF2, IL1R1, INTS4, MAD2L1, PIGU, PIKFYVE, PNRC2, PRKRIR, PRIM2, RNF19A, SDHD, SGOL2, SLC30A7, TMPO, UBE2E1, VAC14 and WDR74 were downregulated, whereas Tmprss6 was upregulated. Concordant with HMVECs, mouse tissue possessed downregulated expression of mRNAs of CAND1, PPP1CC, SH2D1A, SH3BP2, SLC22A5, and TGM2 and upregulated expression of HIST1H3F after exposure for one month. After six months, the expression of HIST1H2AL was upregulated, while TFEC expression was downregulated. Twelve months of exposure led to downregulated expression of ABCE1, EIF4B, IKZF2, IL1R1, LXN, NPM1, PIKFYVE, PPP1CC, SDHD, SLC30A7, SMARCAD1, UBE2E1 and ZC3H13 in addition to upregulated expression of MID1 and NUDT8. Among mouse blood and SAEC, CFTR, PER1, RIMKLB, SH3RF3, and SLC7A1 mRNA expression was downregulated, whereas HSD17B2 expression was upregulated concordantly after one month of exposure. The expression of HMGB2 and SYTL3 mRNAs was downregulated after 6 and 12 months, respectively. Concordant mRNAs between mouse blood and HMVECs after one month of exposure were PER1, SLC22A5 (downregulated) and TUBA1B (upregulated). Six months after exposure, HIST1H3H, KPRP, KRT79 and SHCBP1 expression was upregulated, whereas MID1 expression was downregulated. miR-183, miR-204 and miR-335 were concordant between mouse tissue and SAEC after 1, 6 and 12 months, respectively. In mouse tissue and HMVECs, miR-204 was observed after 6 months, whereas miR-335 and miR-26b were observed after exposure for 12 months. Concordant with mouse blood, after one month of exposure, miR-148b and miR-29c were observed in SAECs and HMVECs, respectively.<sup>89</sup>

Additionally, MWCNTs treated at a dose of  $10 \mu\text{g}/\text{cm}^2$  enhanced the proliferation rate of Met-5A mesothelial cells at G1 phase with enriched migratory and invasive properties after longer durations of exposure. Alterations in the expression of cancer-specific proteins such as PIK3R3, WNT2B, VANGL2 and ANXA1 were observed after treatment with MWCNTs indicating their oncogenic potential. The cells switched to apoptosis resistance after one year of exposure.<sup>90</sup> In another report featuring the same cell line and dose of MWCNTs, the expression of miRNAs such as hsa-miR-155 (upregulated), hsa-miR-30d-5p, hsa-miR-34c-5p, hsa-miR-28-5p and hsa-miR-324-5p (downregulated) were altered. These altered miRNAs have the ability to target the genes engaged in TGF- $\beta$  signaling.<sup>91</sup> Likewise, MWCNTs ( $3.86 \mu\text{m}$  long and  $49 \pm 13.4 \text{ nm}$  wide) at a dose of  $1.2 \mu\text{g}/\text{ml}$  increased the production of ROS in SAEC, improved its ability to migrate and induced phosphorylation of tyrosine and threonine. Among a set of genes analyzed in association with lung inflammation, fibrosis and prospective carcinogenesis, 24 genes were downregulated and 29 genes were upregulated after exposure to MWCNTs. Notably, the expression levels of genes such as Bcl2, Cav1, Cdh4, Dhh, Gpx3, Nos1, Pik3r1, Ptch1, Wif1 and Xpo1 were downregulated, whereas, the expression levels of Ccdc99, Ccl2, Ckap2, Gli1, Nos2, Prmt1, Shh, Sod2 and Tal2 were upregulated. The expression of proteins considered markers of inflammation, such as CCL2 and VEGFA, was greater than that in the control.<sup>92</sup>

Remarkably, serum peptide fractions of male C57BL/6 J mice exposed to MWCNTs (average length of  $3.86 \mu\text{m}$  and diameter of  $49 \text{ nm}$ ) via oropharyngeal aspiration were cocultured with naive endothelial cells. After this procedure, the expression levels of inflammation-related markers Ccl2, Vcam1, Icam1, Tnfa and Tgfb were elevated. The serum fractions are expected to involve or engage a set of integrin-binding proteins (Col2a1, Fbn1 and Lama5) and cell-surface ligands such as galectin 3 along with MMP9 for such effects.<sup>93</sup>

## In vivo Reports for the Safety Profiling of CNTs

The complexes made using  $200 \mu\text{L}$  of SWCNTs with single strands of DNA (ssCTTC3TTC-(9,4),  $2.3 \text{ mg}/\text{L}$ ) were biocompatible and accumulated with higher specificity in the livers of male C57BL/6 mice. The complex was released from the liver 1 h post-injection. Although the tissue sections of all major organs showed the distribution of CNTs, with

the liver and spleen displaying a higher prevalence, no abnormal findings were obtained by histology. CNTs were not prevalent in tissues other than the liver, spleen or kidneys 3 months after being administered. The differences in body weights, blood parameters, and renal and liver biomarkers were insignificant even after over the 5-month period. However, the levels of alkaline phosphatase, chloride and potassium differed slightly. This study relates to the limited or neutral toxicity of CNTs and suggests that these materials are effective in drug delivery or therapy.<sup>94</sup>

MWCNTs (200 nm in length, outer diameters of 30 to 40 nm and inner diameters of 10 nm) loaded with cisplatin (4 mg/kg) were administered to female BALB/c mice for analysis of their biodistribution. The CNTs were more widely distributed in the lungs and spleen than in other major organs after 24 h of intravenous tail injection. The distribution of cisplatin-loaded CNTs was elevated to 14.4% after 1 h compared with 0.7% of the free drug after the same duration. This percentage of accumulation decreased to 9.9% after 4 h. The serum levels of the proinflammatory cytokine IL-1 $\beta$  were higher after 4 h and declined after 24 h. The histological sections showed no abnormalities of vital organs even after the distribution of cisplatin through CNTs after 24 h.<sup>95</sup> It is also encouraging to note that MWCNTs loaded with antitumor agents such as doxorubicin (5 mg/kg) did not induce any systemic toxicity (cardio-, hepato- or nephrotoxicity) in female Sprague-Dawley rats.<sup>29</sup> Furthermore, MWCNTs (5 mg/kg) loaded with glycoproteins were less toxic toward the lungs of rats compared with standard anticancer drugs as observed through the levels of markers for lung toxicity and lung pathology.<sup>28</sup>

## Factors to Be Considered for Reducing the Toxic Effects of CNTs

### Functionalization

Although CNTs have a high surface area which could help in loading larger biological cargos, their surfaces do portray hydrophobicity and narrow solubility in aqueous medium. This attribute can promote their lethal effects on living cells or tissues. These toxic effects mediated by CNTs via the generation of ROS, apoptosis, granulomas and responses linked to inflammation could be effectively neutralized by functionalizing these nanomaterials and reviewing their dimensions. The long surface area and nanoneedle morphology of CNTs endow them with easy access to mobilize across the plasma membrane.<sup>96</sup> Accordingly, surface functionalization with specific compounds or groups can lead to limited toxicity compared with other functional groups. For instance, functionalization with amino groups has been shown to reveal more toxic effects *in vivo*, including loss in body weight than functionalization with the carboxylic groups. This demonstrates that carboxylic-functionalization is relatively safer than amino-functionalization. Additionally, MWCNTs were more toxic when matched with the SWCNTs.<sup>97</sup>

For covalent binding of substances to CNTs, they must be functionalized first with carboxylic groups preferably and shortened in dimensions by ultrasonication. Among the chemical methods of functionalization used to oxidize CNTs, direct fluorination, organic-free radical addition and fluorine displacement are the most commonly preferred. Diimide-activated amidation is another important method for functionalization and improvement of the solubility of CNTs. The functionalized CNTs are characterized by methods such as UV-vis-near IR spectrometry, fluorescence imaging, Fourier transform infrared spectroscopy, surface-enhanced IR absorption, Raman spectroscopy and X-ray photoelectron spectroscopy. In addition, microscopic techniques such as transmission electron microscopy, scanning electron microscopy and atomic force microscopy are adopted.<sup>98</sup>

Overall, the functionalization of CNTs improves their biocompatibility and solubility and minimizes the toxic effects. The duration and dose of CNTs determine their cytotoxicity based on structure, size and the molecules used for functionalization. CNTs can enter mammalian cells easily without any support from external agents.<sup>99–103</sup> The possible rationale underlying the limited toxicity of CNTs after functionalization could be linked to their improved hydrophilic behavior. Surface functionalization can increase their solubility in water, enhance their biocompatibility and prevent the van der Waals force-mediated aggregation of the tubes from occurring.<sup>104</sup> Specifically, covalent functionalization of CNTs is more suitable for their use in nanomedicine as they are more stable than the noncovalently functionalized CNTs *in vivo*. Moreover, CNTs accumulate in different organs of the body and this accumulation is organ-dependent.<sup>105</sup>

Interestingly, tubulins can form functional coatings with MWCNTs, which can be useful in drug delivery across selected destinations. This can be performed by exploiting the organized tubulin confinement and retention of biorecognizing abilities of tubulins for superior assemblies at the nanoscale. It is exciting to note that these tubulin-CNT conjugates can retain the

native functions of tubulins with the ability to polymerize into microtubules. The emanating of protofilaments with neighboring nanotubes or protofilaments can result in the formation of larger bundles around CNTs.<sup>106</sup> This is one example of a possible strategy for enhancing the functionalization, structure or size determination, specific targeting and improved drug delivery into the tumor environment. In association with this study, the biocompatibility of small-molecule drugs improved after being loaded with MWCNTs, and the synergism can help to reduce the toxic effects of MWCNTs.<sup>107</sup>

## Tube Dimensions and Dose

Low quantities of MWCNTs interact with actin filaments or microtubules, whereas higher doses may directly enter the entire cell as well as the nucleus. Treatment with MWCNTs can result in apoptosis via the activation of the spindle network, causing cell cycle arrest at mitosis and the inhibition of DNA synthesis in these cells. In addition, MWCNTs can impede the migration and phagocytic ability of immune cells such as microglia, based on the dose.<sup>108</sup> In addition, the length of CNTs is another critical parameter in CNT-mediated toxicity as long MWCNTs are more toxic than their shorter counterparts.<sup>109</sup> Likewise, the diameter of CNTs is another important factor in determining their toxicity, where CNTs with larger diameters exhibit higher toxic effects.<sup>110</sup>

## Routes of Administration

Drugs are usually administered to animal models through parenteral (intravenous and subcutaneous), intraperitoneal and oral routes. Each route has its own merits for therapeutic benefit.<sup>111</sup> Although the intravenous route results in 100% bioavailability and quick inception of drug action, it results in higher adverse effects compared with the subcutaneous and oral routes.<sup>112,113</sup> The subcutaneous route has several advantages at the clinical level, as it is cost-effective, applies a static dose irrelevant to the body weight and provides the ease of self-administration.<sup>114</sup> Compared with the parenteral routes mentioned above, the oral route is noninvasive and poses the ease of drug intake and patient compliance.<sup>115</sup> The intratumoral route has grown recently as drugs can be carried easily into the tumor site by-passing the systemic off-target adverse effects. Additionally, this route enhances the ability of drugs to effectively attract immune cells to the tumor environment. However, it is difficult to predict the dose, and the route of administration remains elusive for each type of cancer and the patient.<sup>116</sup>

The administration of the intended drug to the nearest site of the tumor seems to be the best route for targeted drug delivery and reduced systemic toxicity. Since drug delivery through the pulmonary route for lung cancer is more intratumoral than other routes and is noninvasive, it adheres to patient compliance and significantly reduces the systemic side effects. The drug is administered directly to the lung or in its close proximity and is absorbed rapidly. This route is therefore efficient in drug delivery for lung cancer and is widely preferred. Among the pulmonary delivery routes, pharyngeal aspiration is easy to adhere to compared with intratracheal instillation as it requires technical expertise and is slightly invasive compared with the former route. However, the drug would be deposited in the respiratory tract (trachea and lungs), whereas pharyngeal aspiration leads to a likely deposition of the drug in the oral cavity.<sup>117</sup> Among these two routes, pharyngeal aspiration seems to be more suitable for further trials at the clinical level as it reduces the perioperative and experiment-associated deaths in animal models.<sup>118</sup>

Since pulmonary toxicity is a key issue associated with CNTs, the usage of these materials must be closely monitored with respect to their size, functionalization, dose and route of administration for studies in animal models and for use in clinical therapeutic approaches for lung cancer. Intratumoral delivery has been recommended to be a more suitable route in drug delivery for cancer therapy using CNTs.<sup>119</sup> Since pulmonary delivery relates more to intratumoral delivery of drugs for lung cancer, as the lung is the primary tumor site, this route may be ideal for this type of cancer after studying the toxic outcomes effectively. This could maximize the therapeutic efficacy of the drug while minimizing the toxic effects. In addition, specific targeting using specific functional agents can improve their hydrophilic behavior, and targeting the surface proteins of cancer cells using antibodies conjugated to the CNTs can improve the diagnosis and/or therapeutic efficacy. Moreover, it can prevent normal and healthy cells from dying.<sup>21,23,120,121</sup>

## Biopersistence and Biodegradation

CNTs are known to persist in lungs, leading to injury of the organ. Subchronic exposure of MWCNTs to the lungs of *in vivo* models through inhalation displayed higher retention half times, with the increases in retention being time- and concentration-dependent. The thickness of connective tissues around the alveolar region increased after the exposure.<sup>122</sup> The responses to acute exposures were similar to those to chronic exposures as CNTs can reach the alveoli and pleura.<sup>123–125</sup> In view of creating these lethal effects, smaller MWCNTs are more effective. The persistence of MWCNTs in the airways declined initially from 16% to 4.2% 336 days post-exposure, whereas the burden in the alveolar region increased from 84% to 95.4% over the same period. Larger MWCNTs left the lungs earlier and accounted for the majority of clearance. The aspiration route creates a significantly lower lung burden than the inhalation route as MWCNTs exposed via inhalation agglomerate and accumulate more in the alveolar interstitium of mice, where the chances of clearance are low.<sup>126</sup> Similar results were obtained for SWCNTs, as exposure through aspiration was found to be safer than inhalation.<sup>127</sup>

Since the inherent electromechanical properties and biopersistence of CNTs remain a concern for their use in cancer nanomedicine, efforts to make them more biodegradable are necessary. The biopersistence and biodistribution of CNTs depend on the sum of walls of the tube, their surface properties and functionalization, diameter, dose and route of administration. In this regard, oxidized MWCNTs were found to be susceptible to enzymatic degradation by intracellular components such as macrophages. This led to a reduction in the lengths of the CNTs compared with the untreated CNTs and a concomitant increase in antitumor effects. The biodegradation of CNTs improved considerably after the therapeutic benefit was achieved (after 7 days).<sup>119</sup> Similarly, the basic amino acids of myeloperoxidase intermediates produced by neutrophils catalyse the biodegradation of SWCNTs by reacting with their carboxyl groups. The biodegraded CNTs did not trigger any proinflammatory responses after being administered into the lungs of mice through pharyngeal aspiration at a dose of 40 µg/mouse.<sup>128</sup> In addition, functionalization with antibodies can improve the biodegradability of CNTs. The functionalization of CNTs results in an enhanced release of myeloperoxidase and formation of peroxynitrite (ROS) by macrophages, which can create favorable materials for degradation. The released enzymes and ions can oxidize SWCNTs into shorter oxidative tubes.<sup>129</sup> Along with myeloperoxidase and peroxynitrites, plant and animal peroxidases have also been suggested to be used for improving the biodegradation and biocompatibility of CNTs.<sup>130</sup>

## Conclusions and Future Perspectives

Nanomedicine for the management of lung cancer is a budding area of research. Among nanomaterials, CNTs remain critical components in the field of drug delivery and cancer therapy, where they act as carriers for several biological macromolecules and proteins. Although CNTs have intrinsic antitumor properties, they are conjugated with standard anticancer drugs to improve their therapeutic efficacy. Although their applications seem intense, due to their dimensions, MWCNTs interact with microtubules, whereas SWCNTs interact with nucleic acids. These interactions lead to genotoxic and/or carcinogenic effects via clastogenic and aneugenic behavior. Collagen deposition, pulmonary inflammation, fibrosis and granulomas are the effects related to the pulmonary toxicity of CNTs. Other effects, such as cholestasis of the liver, were also observed.

The toxic effects produced by CNTs are dependent on their physicochemical and surface properties such as length and diameter, functionalization, dose and route of administration. CNTs with short lengths and diameters functionalized preferably with carboxyl groups, hydrophilic behavior and enhanced biodegradability are considered ideal for drug delivery or therapy. For this purpose, prospective CNTs should be engineered for better applications and limited toxicity.<sup>131</sup> Synthesis methods that focus on the preparation of CNTs with better physicochemical properties are needed to accomplish this.<sup>132</sup> Also, the compatibility of CNTs can be improved by creating oxidized tubes that exhibit enhanced biodegradative potential and limited biopersistence.

There have been significant preclinical attempts to determine the use of CNTs in drug delivery, their therapeutic efficacy and their safety. However, no clinical trials have been conducted on the use of CNTs for cancer therapy to date, and this field seems to still be in its infancy. Hence, the prospects of their clinical usage are to be ascertained by approaches that can allow extensive analyses of their biological effects *in vitro* or *in vivo* in animal models before a proper trial at the clinical stage can be conducted. Their physicochemical and electromechanical profiles have to be

critically reviewed for this purpose. Hence, further research is warranted to modify their carcinogenic potential and limit the undesirable toxic effects associated with their use, thereby increasing the therapeutic index.

## Abbreviations

8-oxodG, 8-Oxo-2'-deoxyguanosine; ABCE1, ATP-binding cassette sub-family E member 1; ADH5, Alcohol Dehydrogenase 5; ALT, alanine aminotransferase; ANLN, Anillin, Actin Binding Protein; ANXA1, Annexin A1; ARF1, ADP Ribosylation Factor 1; AST, aspartate aminotransferase; CAND1, Cullin-associated and neddylation-dissociated 1 protein; CAV1, Caveolin 1; CCDC115, Coiled-Coil Domain Containing 115; Cdc99, Human Coiled Coil Domain Containing Protein 99; CCL2, monocyte chemoattractant protein-1; CCL3, Chemokine (C-C motif) ligand 3; CDH4, Cadherin; CFTR, cystic fibrosis transmembrane conductance regulator; CKAP2, Cytoskeleton Associated Protein 2; CNTs, Carbon nanotubes; COL2A1, Collagen Type II Alpha 1 Chain; CYCS, Cytochrome C, Somatic; DDX24, DEAD-Box Helicase 24; DENND5B, DENN Domain Containing 5B; E-cad, E-cadherin; EIF4B, Eukaryotic Translation Initiation Factor 4B; EMT, Epithelial-Mesenchymal Transition; EPR, enhanced permeability and retention; FBN1, Fibrillin 1; GLI1, GLI Family Zinc Finger 1; GPX3, Glutathione Peroxidase 3; HedA, hydroxyethylidA; HedG, hydroxyethylidG; HedU, hydroxyethylidU; HIST1H2AL, Histone H2A type 1; HMGB2, High Mobility Group Box 2; HMVECs, Human Microvascular Endothelial Cells; HS3ST3B1, Heparan Sulfate-Glucosamine 3-Sulfotransferase 3B1; HSD17B2, Hydroxysteroid 17-Beta Dehydrogenase 2; IFN- $\gamma$ , Interferon gamma; IKZF2, IKAROS Family Zinc Finger 2; IL1R1, Interleukin 1 Receptor Type 1; INTS4, Integrator Complex Subunit 4; KIF14, Kinesin Family Member 14; KPRP, Keratinocyte Proline Rich Protein; KRT79, Keratin 79; LAMA5, Laminin Subunit Alpha 5; LDH, Lactate dehydrogenase; LXRs, Liver X Receptors; MAD2L1, mitotic arrest deficient 2 like 1; MAML1, Mastermind-Like Transcriptional Coactivator 1; MAN2B2, Mannosidase Alpha Class 2B Member 2; MCP-1, monocyte chemoattractant protein-1; METTL21, Methyltransferase-like 21; MIP-2, Macrophage Inflammatory Protein 2; MMP, matrix metalloproteinase; MTs, mutant frequencies; MWCNTs, multi-walled carbon nanotubes; MYBPC2, Myosin Binding Protein C2; N-cad, N-cadherin; NOS1, Nitric Oxide Synthase 1; NPM1, Nucleophosmin 1; NSCLC, non-small cell lung cancer; NUDT8, Nudix Hydrolase 8; PER1, Period Circadian Regulator 1; PIGU, Phosphatidylinositol Glycan Anchor Biosynthesis Class U; PIK3R3, Phosphoinositide-3-Kinase Regulatory Subunit 3; PIKFYVE, Phosphoinositide Kinase, FYVE-Type Zinc Finger Containing; PMNs, polymorphonuclear neutrophils; PNR2, Proline Rich Nuclear Receptor Coactivator 2; PPP1C, protein phosphatase 1 catalytic subunit gamma; PRIM2, DNA Primase Subunit 2; PRMT1, Protein Arginine Methyltransferase 1; PTCH1, Patched 1; RIMKLB, Ribosomal Modification Protein RimK Like Family Member B; RNF19A, Ring Finger Protein 19A, RBR E3 Ubiquitin Protein Ligase; ROS, reactive oxygen species; RXRs, Retinoid X Receptors; S100A5, S100 Calcium Binding Protein A5; SAEC, Small Airway Epithelial Cells; SCLC, small cell lung cancer; SDHD, Succinate Dehydrogenase Complex Subunit D; SEM, Scanning electron microscopy; SGOL2, Shugoshin-like 2; SH2D1A, SH2 domain-containing protein 1A; SH3BP2, SH3 Domain Binding Protein 2; SH3RF3, SH3 Domain Containing Ring Finger 3; SHCBP1, SHC Binding and Spindle Associated 1; SHH, Sonic Hedgehog Signaling Molecule; sICAM-1, soluble intracellular adhesion molecular 1; siRNA, Small interfering RNA; SLC22A5, Solute Carrier Family 22 Member 5; SLC30A7, Solute Carrier Family 30 Member 7; SLC7A1, Solute Carrier Family 7 Member 1; SMARCA4, SWI/SNF-related matrix-associated actin-dependent regulator of chromatin subfamily A containing DEAD/H box 1; sVCAM-1, soluble vascular cell adhesion molecule 1; SWCNTs, Single-walled carbon nanotubes; SYTL3, Synaptotagmin Like 3; TAL2, TAL BHLH Transcription Factor 2; TEM, Transmission electron microscopy; TFEC, Transcription Factor EC; TGF $\beta$ 1, transforming growth factor beta 1; TGM2, Transglutaminase 2; TIMP-1, tissue inhibitor of metalloproteinase-1; TMPO, Thymopoietin; TNF- $\alpha$ , tumor necrosis factor alpha; TTF-1, thyroid transcription factor-1; TTLL7, Tubulin Tyrosine Ligase Like 7; TUBA1B, Tubulin Alpha 1b; UBE2E1, Ubiquitin Conjugating Enzyme E2 E1; VANGL2, VANGL Planar Cell Polarity Protein 2; VEGF A, vascular endothelial growth factor A; VEGFA, Vascular Endothelial Growth Factor A; WDR74, WD Repeat Domain 74; WHO, World Health Organization; WIF1, WNT Inhibitory Factor 1; WNT2B, Wnt Family Member 2B; Xpo1, Exportin 1; ZC3H13, Zinc Finger CCCH-Type Containing 13; ZO-1, Zonula occludens-1.

## Acknowledgments

This work was supported by The Jiangsu Provincial Bureau of Traditional Chinese Medicine (YB2020070).

## Disclosure

The authors report no conflicts of interest in this work.

## References

1. Nethan S, Sinha D, Mehrotra R. Non communicable disease risk factors and their trends in India. *Asian Pac J Cancer Prev*. 2017;18(7):2005–2010. doi:10.22034/APJCP.2017.18.7.2005
2. Khaltaev N, Axelrod S. Global lung cancer mortality trends and lifestyle modifications: preliminary analysis. *Chin Med J*. 2020;133(13):1526–1532. doi:10.1097/CM9.0000000000000918
3. Countdown NCD, Stevens GA, Mathers CD. 2030: worldwide trends in non-communicable disease mortality and progress towards sustainable development goal target 3.4. *Lancet*. 2018;392(10152):1072–1088. doi:10.1016/S0140-6736(18)31992-5
4. Xia C, Dong X, Li H, et al. Cancer statistics in China and United States, 2022: profiles, trends, and determinants. *Chin Med J*. 2022;135(5):584–590. doi:10.1097/CM9.0000000000002108
5. Siegel RL, Miller KD, Fuchs HE, Jemal A. Cancer statistics, 2022. *CA Cancer J Clin*. 2022;72(1):7–33. doi:10.3322/caac.21708
6. Siddiqui F, Vaqar S, Siddiqui AH. Lung cancer. In: *StatPearls*. Treasure Island (FL): StatPearls Publishing Copyright © 2022, StatPearls Publishing LLC.; 2022.
7. Miller KD, Siegel RL, Lin CC, et al. Cancer treatment and survivorship statistics, 2016. *CA Cancer J Clin*. 2016;66(4):271–289. doi:10.3322/caac.21349
8. García-Fernández C, Fornaguera C, Borrós S. Nanomedicine in non-small cell lung cancer: from conventional treatments to immunotherapy. *Cancers*. 2020;12(6):1609. doi:10.3390/cancers12061609
9. Pandey G, Jain P. Assessing the nanotechnology on the grounds of costs, benefits, and risks. *Beni-Suef Univ J Basic Appl Sci*. 2020;9(1):63. doi:10.1186/s43088-020-00085-5
10. Morigi V, Tocchio A, Bellavite Pellegrini C, Sakamoto JH, Arnone M, Tasciotti E. Nanotechnology in medicine: from inception to market domination. *J Drug Deliv*. 2012;2012:1–7. doi:10.1155/2012/389485
11. Ventola CL. Progress in nanomedicine: approved and investigational nanodrugs. *P T*. 2017;42(12):742–755. doi:10.1155/2015/123756
12. Hussain S. Nanomedicine for treatment of lung cancer. In: *Lung Cancer and Personalized Medicine: Novel Therapies and Clinical Management*. Springer; 2016:137–147.
13. Zare H, Ahmadi S, Ghasemi A, et al. Carbon nanotubes: smart drug/gene delivery carriers. *Int J Nanomedicine*. 2021;16:1681. doi:10.2147/IJN.S299448
14. Herrero-Latorre C, Álvarez-méndez J, Barciela-García J, García-Martín S, Peña-Creciente R. Characterization of carbon nanotubes and analytical methods for their determination in environmental and biological samples: a review. *Anal Chim Acta*. 2015;853:77–94. doi:10.1016/j.aca.2014.10.008
15. Tomada J, Dienel T, Hampel F, Fasel R, Amsharov K. Combinatorial design of molecular seeds for chirality-controlled synthesis of single-walled carbon nanotubes. *Nat Commun*. 2019;10(1):3278. doi:10.1038/s41467-019-11192-y
16. Beg S, Rahman M, Jain A, et al. Chapter 4 - emergence in the functionalized carbon nanotubes as smart nanocarriers for drug delivery applications. In Grumezescu AM, editor. *Fullerens, Graphenes and Nanotubes*. William Andrew Publishing; 2018:105–133.
17. Sakharova NA, Pereira AF, Antunes JM, Fernandes JV. Mechanical characterization of multiwalled carbon nanotubes: numerical simulation study. *Materials*. 2020;13(19):4283. doi:10.3390/ma13194283
18. Parker AL, Kavallaris M, McCarroll JA. Microtubules and their role in cellular stress in cancer. *Front Oncol*. 2014;4:153. doi:10.3389/fonc.2014.00153
19. Pampaloni F, Florin E-L. Microtubule architecture: inspiration for novel carbon nanotube-based biomimetic materials. *Trends Biotechnol*. 2008;26(6):302–310. doi:10.1016/j.tibtech.2008.03.002
20. González-Lavado E, Valdivia L, García-Castaño A, et al. Multi-walled carbon nanotubes complement the anti-tumoral effect of 5-Fluorouracil. *Oncotarget*. 2019;10(21):2022. doi:10.18632/oncotarget.26770
21. Son KH, Hong JH, Lee JW. Carbon nanotubes as cancer therapeutic carriers and mediators. *Int J Nanomedicine*. 2016;11:5163. doi:10.2147/IJN.S112660
22. Elhissi A, Ahmed W, Hassan IU, Dhanak V, D'Emanuele A. Carbon nanotubes in cancer therapy and drug delivery. *J Drug Deliv*. 2012;2012:1–10. doi:10.1155/2012/837327
23. Bura C, Mocan T, Grapa C, Mocan L. Carbon nanotubes-based assays for cancer detection and screening. *Pharmaceutics*. 2022;14(4):781. doi:10.3390/pharmaceutics14040781
24. Tang L, Xiao Q, Mei Y, et al. Insights on functionalized carbon nanotubes for cancer theranostics. *J Nanobiotechnology*. 2021;19(1):423. doi:10.1186/s12951-021-01174-y
25. Kamazani FM, Sotoodehnejad Nematalahi F, Siadat SD, Pornour M, Sheikhpour M. A success targeted nano delivery to lung cancer cells with multi-walled carbon nanotubes conjugated to bromocriptine. *Sci Rep*. 2021;11(1):24419. doi:10.1038/s41598-021-03031-2
26. Morais RP, Novais GB, Sengenito LS, et al. Naringenin-functionalized multi-walled carbon nanotubes: a potential approach for site-specific remote-controlled anticancer delivery for the treatment of lung cancer cells. *Int J Mol Sci*. 2020;21(12):4557. doi:10.3390/ijms21124557
27. Kim S-W, Lee YK, Lee JY, Hong JH, Khang D. PEGylated anticancer-carbon nanotubes complex targeting mitochondria of lung cancer cells. *Nanotechnology*. 2017;28(46):465102. doi:10.1088/1361-6528/aa8c31
28. Singh RP, Sharma G, Singh S, et al. Effects of transferrin conjugated multi-walled carbon nanotubes in lung cancer delivery. *Mater Sci Eng C*. 2016;67:313–325. doi:10.1016/j.msec.2016.05.013
29. Datir SR, Das M, Singh RP, Jain S. Hyaluronate tethered, “smart” multiwalled carbon nanotubes for tumor-targeted delivery of doxorubicin. *Bioconjug Chem*. 2012;23(11):2201–2213. doi:10.1021/bc300248t
30. Das M, Datir SR, Singh RP, Jain S. Augmented anticancer activity of a targeted, intracellularly activatable, theranostic nanomedicine based on fluorescent and radiolabeled, methotrexate-folic acid-multiwalled carbon nanotube conjugate. *Mol Pharm*. 2013;10(7):2543–2557. doi:10.1021/mp300701e

31. Heger Z, Polanska H, Krizkova S, et al. Co-delivery of VP-16 and Bcl-2-targeted antisense on PEG-grafted oMWCNTs for synergistic in vitro anti-cancer effects in non-small and small cell lung cancer. *Colloids Surf B Biointerfaces*. 2017;150:131–140. doi:10.1016/j.colsurfb.2016.11.023
32. Lodhi N, Mehra NK, Jain NK. Development and characterization of dexamethasone mesylate anchored on multi walled carbon nanotubes. *J Drug Target*. 2013;21(1):67–76. doi:10.3109/1061186X.2012.729213
33. Salas-Treviño D, Saucedo-Cárdenas O, Loera-Arias MJ, et al. Hyaluronate functionalized multi-wall carbon nanotubes filled with carboplatin as a novel drug nanocarrier against murine lung cancer cells. *Nanomaterials*. 2019;9(11):1572. doi:10.3390/nano9111572
34. Qi Y, Yang W, Liu S, et al. Cisplatin loaded multiwalled carbon nanotubes reverse drug resistance in NSCLC by inhibiting EMT. *Cancer Cell Int*. 2021;21(1):1–11. doi:10.1186/s12935-021-01771-9
35. Singh N, Sachdev A, Gopinath P. Polysaccharide functionalized single walled carbon nanotubes as nanocarriers for delivery of curcumin in lung cancer cells. *J Nanosci Nanotechnol*. 2018;18(3):1534–1541. doi:10.1166/jnn.2018.14222
36. Yu B, Tan L, Zheng R, Tan H, Zheng L. Targeted delivery and controlled release of Paclitaxel for the treatment of lung cancer using single-walled carbon nanotubes. *Mater Sci Eng C*. 2016;68:579–584. doi:10.1016/j.msec.2016.06.025
37. Arya N, Arora A, Vasu K, Sood AK, Katti DS. Combination of single walled carbon nanotubes/graphene oxide with paclitaxel: a reactive oxygen species mediated synergism for treatment of lung cancer. *Nanoscale*. 2013;5(7):2818–2829. doi:10.1039/c3nr33190c
38. Hitoshi K, Katoh M, Suzuki T, Ando Y, Nadai M. Differential effects of single-walled carbon nanotubes on cell viability of human lung and pharynx carcinoma cell lines. *J Toxicol Sci*. 2011;36(3):379–387. doi:10.2131/jts.36.379
39. Cao Y, Huang H-Y, Chen L-Q, et al. Enhanced lysosomal escape of pH-responsive polyethylenimine–betaine functionalized carbon nanotube for the codelivery of survivin small interfering RNA and doxorubicin. *ACS Appl Mater Interfaces*. 2019;11(10):9763–9776. doi:10.1021/acsami.8b20810
40. Razzazan A, Atyabi F, Kazemi B, Dinarvand R. In vivo drug delivery of gemcitabine with PEGylated single-walled carbon nanotubes. *Mater Sci Eng C*. 2016;62:614–625. doi:10.1016/j.msec.2016.01.076
41. Zakaria AB, Picaud F, Rattier T, et al. Nanovectorization of TRAIL with single wall carbon nanotubes enhances tumor cell killing. *Nano Lett*. 2015;15(2):891–895. doi:10.1021/nl503565t
42. Ghosh M, Das PK. Doxorubicin loaded 17 $\beta$ -estradiol based SWNT dispersions for target specific killing of cancer cells. *Colloids Surf B Biointerfaces*. 2016;142:367–376. doi:10.1016/j.colsurfb.2016.03.005
43. Hassan HA, Smyth L, Wang JT-W, et al. Dual stimulation of antigen presenting cells using carbon nanotube-based vaccine delivery system for cancer immunotherapy. *Biomaterials*. 2016;104:310–322. doi:10.1016/j.biomaterials.2016.07.005
44. Guo C, Al-Jamal WT, Toma FM, et al. Design of cationic multiwalled carbon nanotubes as efficient siRNA vectors for lung cancer xenograft eradication. *Bioconjug Chem*. 2015;26(7):1370–1379. doi:10.1021/acs.bioconjchem.5b00249
45. Podesta JE, Al-Jamal KT, Herrero MA, et al. Antitumor activity and prolonged survival by carbon-nanotube-mediated therapeutic siRNA silencing in a human lung xenograft model. *Small*. 2009;5(10):1176–1185. doi:10.1002/sml.200801572
46. Yang M, Meng J, Cheng X, et al. Multiwalled carbon nanotubes interact with macrophages and influence tumor progression and metastasis. *Theranostics*. 2012;2(3):258. doi:10.7150/thno.3629
47. González-Domínguez E, Iturriz-Rodríguez N, Padin-Gonzalez E, et al. Carbon nanotubes gathered onto silica particles lose their biomimetic properties with the cytoskeleton becoming biocompatible. *Int J Nanomedicine*. 2017;12:6317. doi:10.2147/IJN.S141794
48. García-Hevia L, Valiente R, Fernández-Luna JL, et al. Inhibition of cancer cell migration by multiwalled carbon nanotubes. *Adv Healthcare Mater*. 2015;4(11):1640–1644. doi:10.1002/adhm.201500252
49. Rodríguez-Fernández L, Valiente R, Gonzalez J, Villegas JC, Fanarraga ML. Multiwalled carbon nanotubes display microtubule biomimetic properties in vivo, enhancing microtubule assembly and stabilization. *ACS Nano*. 2012;6(8):6614–6625. doi:10.1021/nn302222m
50. Srivastava RK, Pant AB, Kashyap MP, et al. Multi-walled carbon nanotubes induce oxidative stress and apoptosis in human lung cancer cell line-A549. *Nanotoxicology*. 2011;5(2):195–207. doi:10.3109/17435390.2010.503944
51. García-Hevia L, Villegas JC, Fernández F, et al. Multiwalled carbon nanotubes inhibit tumor progression in a mouse model. *Adv Healthcare Mater*. 2016;5(9):1080–1087. doi:10.1002/adhm.201500753
52. Hevia LG, Fanarraga ML. Microtubule cytoskeleton-disrupting activity of MWCNTs: applications in cancer treatment. *J Nanobiotechnol*. 2020;18(1):181. doi:10.1186/s12951-020-00742-y
53. Umemura K. Hybrids of Nucleic acids and carbon nanotubes for nanobiotechnology. *Nanomaterials*. 2015;5(1):321–350. doi:10.3390/nano5010321
54. Ma J, Wang J-N, Tsai C-J, Nussinov R, Ma B. Diameters of single-walled carbon nanotubes (SWCNTs) and related nanochemistry and nanobiology. *Front Mater Sci China*. 2010;4(1):17–28. doi:10.1007/s11706-010-0001-8
55. Wu Y, Phillips JA, Liu H, Yang R, Tan W. Carbon nanotubes protect DNA strands during cellular delivery. *ACS Nano*. 2008;2(10):2023–2028. doi:10.1021/nn800325a
56. Singh R, Pantarotto D, McCarthy D, et al. Binding and condensation of plasmid DNA onto functionalized carbon nanotubes: toward the construction of nanotube-based gene delivery vectors. *J Am Chem Soc*. 2005;127(12):4388–4396. doi:10.1021/ja0441561
57. Pantarotto D, Singh R, McCarthy D, et al. Functionalized carbon nanotubes for plasmid DNA gene delivery. *Angewandte Chemie*. 2004;43(39):5242–5246. doi:10.1002/anie.200460437
58. Zhang Z, Yang X, Zhang Y, et al. Delivery of telomerase reverse transcriptase small interfering RNA in complex with positively charged single-walled carbon nanotubes suppresses tumor growth. *Clin Cancer Res*. 2006;12(16):4933–4939. doi:10.1158/1078-0432.CCR-05-2831
59. Varkouhi AK, Foillard S, Lammers T, et al. siRNA delivery with functionalized carbon nanotubes. *Int J Pharm*. 2011;416(2):419–425. doi:10.1016/j.ijpharm.2011.02.009
60. Shi Kam NW, Jessop TC, Wender PA, Dai H. Nanotube molecular transporters: internalization of carbon nanotube-protein conjugates into mammalian cells. *J Am Chem Soc*. 2004;126(22):6850–6851. doi:10.1021/ja0486059
61. Zhang W, Ding Q, Jinruan J, Fang J. Biomolecular interactions and application of carbon nanotubes in nanomedicine. *Austin Biomol*. 2016;1:1005.
62. Chen Y, Qu K, Zhao C, et al. Insights into the biomedical effects of carboxylated single-wall carbon nanotubes on telomerase and telomeres. *Nat Commun*. 2012;3(1):1074. doi:10.1038/ncomms2091

63. Wolski P, Wojton P, Nieszporek K, Panczyk T. Interaction of human telomeric i-motif DNA with single-walled carbon nanotubes: insights from molecular dynamics simulations. *J Phys Chem B*. 2019;123(49):10343–10353. doi:10.1021/acs.jpcc.9b07292
64. Snyder-Talkington BN, Schwegler-Berry D, Castranova V, Qian Y, Guo NL. Multi-walled carbon nanotubes induce human microvascular endothelial cellular effects in an alveolar-capillary co-culture with small airway epithelial cells. *Part Fibre Toxicol*. 2013;10(1):1–14. doi:10.1186/1743-8977-10-35
65. Polimeni M, Gulino GR, Gazzano E, et al. Multi-walled carbon nanotubes directly induce epithelial-mesenchymal transition in human bronchial epithelial cells via the TGF- $\beta$ -mediated Akt/GSK-3 $\beta$ /SNAIL-1 signalling pathway. *Part Fibre Toxicol*. 2015;13(1):1–19. doi:10.1186/s12989-016-0138-4
66. Wang P, Wang Y, Nie X, Braïni C, Bai R, Chen C. Multiwall carbon nanotubes directly promote fibroblast–myofibroblast and epithelial–mesenchymal transitions through the activation of the TGF- $\beta$ /Smad signaling pathway. *Small*. 2015;11(4):446–455. doi:10.1002/sml.201303588
67. Wang P, Nie X, Wang Y, et al. Multiwall carbon nanotubes mediate macrophage activation and promote pulmonary fibrosis through TGF- $\beta$ /Smad signaling pathway. *Small*. 2013;9(22):3799–3811. doi:10.1002/sml.201300607
68. Kinaret P, Ilves M, Fortino V, et al. Inhalation and oropharyngeal aspiration exposure to rod-like carbon nanotubes induce similar airway inflammation and biological responses in mouse lungs. *ACS Nano*. 2017;11(1):291–303. doi:10.1021/acsnano.6b05652
69. Park E-J, Cho W-S, Jeong J, Yi J, Choi K, Park K. Pro-inflammatory and potential allergic responses resulting from B cell activation in mice treated with multi-walled carbon nanotubes by intratracheal instillation. *Toxicology*. 2009;259(3):113–121. doi:10.1016/j.tox.2009.02.009
70. van Berlo D, Wilhelmi V, Boots AW, et al. Apoptotic, inflammatory, and fibrogenic effects of two different types of multi-walled carbon nanotubes in mouse lung. *Arch Toxicol*. 2014;88(9):1725–1737. doi:10.1007/s00204-014-1220-z
71. Shvedova A, Kisin E, Murray A, et al. ESR evidence for in vivo formation of free radicals in tissue of mice exposed to single-walled carbon nanotubes. *Free Radic Biol Med*. 2014;73:154–165. doi:10.1016/j.freeradbiomed.2014.05.010
72. Ge C, Meng L, Xu L, et al. Acute pulmonary and moderate cardiovascular responses of spontaneously hypertensive rats after exposure to single-wall carbon nanotubes. *Nanotoxicology*. 2012;6(5):526–542. doi:10.3109/17435390.2011.587905
73. Principi E, Girardello R, Bruno A, et al. Systemic distribution of single-walled carbon nanotubes in a novel model: alteration of biochemical parameters, metabolic functions, liver accumulation, and inflammation in vivo. *Int J Nanomedicine*. 2016;11:4299. doi:10.2147/IJN.S109950
74. Fukai E, Sato H, Watanabe M, Nakae D, Totsuka Y. Establishment of an in vivo simulating co-culture assay platform for genotoxicity of multi-walled carbon nanotubes. *Cancer Sci*. 2018;109(4):1024–1031. doi:10.1111/cas.13534
75. Siegrist KJ, Reynolds SH, Porter DW, et al. Mitsui-7, heat-treated, and nitrogen-doped multi-walled carbon nanotubes elicit genotoxicity in human lung epithelial cells. *Part Fibre Toxicol*. 2019;16(1):1–19. doi:10.1186/s12989-019-0318-0
76. Snyder-Talkington BN, Dong C, Zhao X, et al. Multi-walled carbon nanotube-induced gene expression in vitro: concordance with in vivo studies. *Toxicology*. 2015;328:66–74. doi:10.1016/j.tox.2014.12.012
77. Muller J, Decordier I, Hoet PH, et al. Clastogenic and aneugenic effects of multi-wall carbon nanotubes in epithelial cells. *Carcinogenesis*. 2008;29(2):427–433. doi:10.1093/carcin/bgm243
78. Stueckle TA, Davidson DC, Derk R, et al. Effect of surface functionalizations of multi-walled carbon nanotubes on neoplastic transformation potential in primary human lung epithelial cells. *Nanotoxicology*. 2017;11(5):613–624. doi:10.1080/17435390.2017.1332253
79. Kato T, Totsuka Y, Ishino K, et al. Genotoxicity of multi-walled carbon nanotubes in both in vitro and in vivo assay systems. *Nanotoxicology*. 2013;7(4):452–461. doi:10.3109/17435390.2012.674571
80. Saleh DM, Luo S, Ahmed OHM, et al. Assessment of the toxicity and carcinogenicity of double-walled carbon nanotubes in the rat lung after intratracheal instillation: a two-year study. *Part Fibre Toxicol*. 2022;19(1):1–21. doi:10.1186/s12989-022-00469-8
81. Rittinghausen S, Hackbarth A, Creutzenberg O, et al. The carcinogenic effect of various multi-walled carbon nanotubes (MWCNTs) after intraperitoneal injection in rats. *Part Fibre Toxicol*. 2014;11(1):1–18. doi:10.1186/s12989-014-0059-z
82. Sargent LM, Hubbs AF, Young SH, et al. Single-walled carbon nanotube-induced mitotic disruption. *Mutat Res*. 2012;745(1–2):28–37. doi:10.1016/j.mrgentox.2011.11.017
83. Li X, Peng Y, Qu X. Carbon nanotubes selective destabilization of duplex and triplex DNA and inducing B–A transition in solution. *Nucleic Acids Res*. 2006;34(13):3670–3676. doi:10.1093/nar/gkl513
84. Cveticanin J, Joksic G, Leskovic A, Petrovic S, Sobot AV, Neskovic O. Using carbon nanotubes to induce micronuclei and double strand breaks of the DNA in human cells. *Nanotechnology*. 2009;21(1):015102. doi:10.1088/0957-4484/21/1/015102
85. Voronkova MA, Luanpitpong S, Rojanasakul LW, et al. SOX9 regulates cancer stem-like properties and metastatic potential of single-walled carbon nanotube-exposed cells. *Sci Rep*. 2017;7(1):1–13. doi:10.1038/s41598-017-12037-8
86. Wang P, Voronkova M, Luanpitpong S, et al. Induction of slug by chronic exposure to single-walled carbon nanotubes promotes tumor formation and metastasis. *Chem Res Toxicol*. 2017;30(7):1396–1405. doi:10.1021/acs.chemrestox.7b00049
87. Luanpitpong S, Wang L, Castranova V, Rojanasakul Y. Induction of stem-like cells with malignant properties by chronic exposure of human lung epithelial cells to single-walled carbon nanotubes. *Part Fibre Toxicol*. 2014;11(1):1–18. doi:10.1186/1743-8977-11-22
88. Wang J, Tian X, Zhang J, et al. Postchronic single-walled carbon nanotube exposure causes irreversible malignant transformation of human bronchial epithelial cells through DNA methylation changes. *ACS Nano*. 2021;15(4):7094–7104. doi:10.1021/acsnano.1c00239
89. Snyder-Talkington BN, Dong C, Singh S, et al. Multi-walled carbon nanotube-induced gene expression biomarkers for medical and occupational surveillance. *Int J Mol Sci*. 2019;20(11):2635. doi:10.3390/ijms20112635
90. Ju L, Yu M, Zhu L, Jia Z, Zhang M, Chen J. Chronic toxicity of Multi-walled carbon nanotubes in human pleural mesothelial cells. *Zhonghua Lao Dong Wei Sheng Zhi Ye Bing Za Zhi*. 2021;39(3):173–177. doi:10.3760/cma.j.cn121094-20190919-00382
91. Yin X, Ju L, Wu W, et al. Changes of microRNAs profiling in mesothelial cells exposed to multi-walled carbon nanotubes. *Zhonghua Lao Dong Wei Sheng Zhi Ye Bing Za Zhi*. 2016;34(7):531–534. doi:10.3760/cma.j.issn.1001-9391.2016.07.014
92. Snyder-Talkington BN, Pacurari M, Dong C, et al. Systematic analysis of multiwalled carbon nanotube-induced cellular signaling and gene expression in human small airway epithelial cells. *Toxicol Sci*. 2013;133(1):79–89. doi:10.1093/toxsci/kft019
93. Mostovenko E, Young T, Muldoon PP, et al. Nanoparticle exposure driven circulating bioactive peptidome causes systemic inflammation and vascular dysfunction. *Part Fibre Toxicol*. 2019;16(1):1–23. doi:10.1186/s12989-019-0304-6

94. Galassi TV, Antman-Passig M, Yaari Z, Jessurun J, Schwartz RE, Heller DA. Long-term in vivo biocompatibility of single-walled carbon nanotubes. *PLoS One*. 2020;15(5):e0226791. doi:10.1371/journal.pone.0226791
95. Li J, Pant A, Chin CF, et al. In vivo biodistribution of platinum-based drugs encapsulated into multi-walled carbon nanotubes. *Nanomedicine*. 2014;10(7):1465–1475. doi:10.1016/j.nano.2014.01.004
96. Chenthamara D, Subramaniam S, Ramakrishnan SG, et al. Therapeutic efficacy of nanoparticles and routes of administration. *Biomater Res*. 2019;23(1):20. doi:10.1186/s40824-019-0166-x
97. Mohammadi E, Zeinali M, Mohammadi-Sardoo M, Iranpour M, Behnam B, Mandegary A. The effects of functionalization of carbon nanotubes on toxicological parameters in mice. *Hum Exp Toxicol*. 2020;39(9):1147–1167. doi:10.1177/0960327119899988
98. Daniel S, Rao TP, Rao KS, et al. A review of DNA functionalized/grafted carbon nanotubes and their characterization. *Sens Actuators B Chem*. 2007;122(2):672–682. doi:10.1016/j.snb.2006.06.014
99. He H, Pham-Huy LA, Dramou P, Xiao D, Zuo P, Pham-Huy C. Carbon nanotubes: applications in pharmacy and medicine. *Biomed Res Int*. 2013;2013:1–12. doi:10.1155/2013/578290
100. Vardharajula S, Ali SZ, Tiwari PM, et al. Functionalized carbon nanotubes: biomedical applications. *Int J Nanomedicine*. 2012;7:5361–5374. doi:10.2147/IJN.S35832
101. Czarnecka J, Wiśniewski M, Forbot N, Bolibok P, Terzyk AP, Roszek K. Cytotoxic or not? Disclosing the toxic nature of carbonaceous nanomaterials through nano–bio interactions. *Materials*. 2020;13(9):2060. doi:10.3390/ma13092060
102. Cui H-F, Vashist SK, Al-Rubeaan K, Luong JH, Sheu F-S. Interfacing carbon nanotubes with living mammalian cells and cytotoxicity issues. *Chem Res Toxicol*. 2010;23(7):1131–1147. doi:10.1021/tx100050h
103. Lamberti M, Pedata P, Sannolo N, Porto S, De Rosa A, Caraglia M. Carbon nanotubes: properties, biomedical applications, advantages and risks in patients and occupationally-exposed workers. *Int J Immunopathol Pharmacol*. 2015;28(1):4–13. doi:10.1177/0394632015572559
104. Khodabandehloo H, Zahednasab H, Ashrafi Hafez A. Nanocarriers usage for drug delivery in cancer therapy. *Iran J Cancer Prev*. 2016;9(2):e3966. doi:10.17795/ijcp-3966
105. Yang S-T, Luo J, Zhou Q, Wang H. Pharmacokinetics, metabolism and toxicity of carbon nanotubes for biomedical purposes. *Theranostics*. 2012;2(3):271. doi:10.7150/thno.3618
106. Dinu CZ, Bale SS, Zhu G, Dordick JS. Tubulin encapsulation of carbon nanotubes into functional hybrid assemblies. *Small*. 2009;5(3):310–315. doi:10.1002/sml.200801434
107. Qi W, Tian L, An W, et al. Curing the toxicity of multi-walled carbon nanotubes through native small-molecule drugs. *Sci Rep*. 2017;7(1):2815. doi:10.1038/s41598-017-02770-5
108. Villegas JC, Álvarez-montes L, Rodríguez-Fernández L, González J, Valiente R, Fanarraga ML. Multiwalled carbon nanotubes hinder microglia function interfering with cell migration and phagocytosis. *Adv Healthcare Mater*. 2014;3(3):424–432. doi:10.1002/adhm.201300178
109. Chen T, Nie H, Gao X, et al. Epithelial-mesenchymal transition involved in pulmonary fibrosis induced by multi-walled carbon nanotubes via TGF-beta/Smad signaling pathway. *Toxicol Lett*. 2014;226(2):150–162. doi:10.1016/j.toxlet.2014.02.004
110. Das R, Leo BF, Murphy F. The Toxic truth about carbon nanotubes in water purification: a perspective view. *Nanoscale Res Lett*. 2018;13(1):183. doi:10.1186/s11671-018-2589-z
111. Al Shoyaib A, Archie SR, Karamyan VT. Intraperitoneal route of drug administration: should it be used in experimental animal studies? *Pharm Res*. 2019;37(1):12. doi:10.1007/s11095-019-2745-x
112. Spahn JD, Szefer SJ. Chapter 16 - pharmacology of the lung and drug therapy. In: Taussig LM, Landau LI, editors. *Pediatric Respiratory Medicine*. Second ed. Philadelphia: Mosby; 2008:219–233.
113. Jonaitis L, Marković S, Farkas K, et al. Intravenous versus subcutaneous delivery of biotherapeutics in IBD: an expert's and patient's perspective. *BMC Proc*. 2021;15(17):25. doi:10.1186/s12919-021-00230-7
114. Bittner B, Richter W, Schmidt J. Subcutaneous administration of biotherapeutics: an overview of current challenges and opportunities. *BioDrugs*. 2018;32(5):425–440. doi:10.1007/s40259-018-0295-0
115. Alqahtani MS, Kazi M, Alsenaidy MA, Ahmad MZ. Advances in oral drug delivery. *Front Pharmacol*. 2021;12:618411. doi:10.3389/fphar.2021.618411
116. Huppert LA, Daud AI. Intratumoral therapies and in-situ vaccination for melanoma. *Hum Vaccin Immunother*. 2022;18(3):1890512. doi:10.1080/21645515.2021.1890512
117. Kunda NK, Price DN, Muttill P. Respiratory tract deposition and distribution pattern of microparticles in mice using different pulmonary delivery techniques. *Vaccines*. 2018;6(3):41. doi:10.3390/vaccines6030041
118. Barbayianni I, Ninou I, Tzouveleakis A, Aidinis V. Bleomycin revisited: a direct comparison of the intratracheal micro-spraying and the oropharyngeal aspiration routes of bleomycin administration in mice. *Front Med*. 2018;5:269. doi:10.3389/fmed.2018.00269
119. González-Lavado E, Iturrioz-Rodríguez N, Padín-González E, et al. Biodegradable multi-walled carbon nanotubes trigger anti-tumoral effects. *Nanoscale*. 2018;10(23):11013–11020. doi:10.1039/C8NR03036G
120. Heister E, Neves V, Tilmaçiu C, et al. Triple functionalisation of single-walled carbon nanotubes with doxorubicin, a monoclonal antibody, and a fluorescent marker for targeted cancer therapy. *Carbon*. 2009;47(9):2152–2160. doi:10.1016/j.carbon.2009.03.057
121. Beckler B, Cowan A, Farrar N, et al. Microwave Heating of antibody-functionalized carbon nanotubes as a feasible cancer treatment. *Biomed Phys Eng Express*. 2018;4(4):045025. doi:10.1088/2057-1976/aac9fe
122. Pauluhn J. Subchronic 13-week inhalation exposure of rats to multiwalled carbon nanotubes: toxic effects are determined by density of agglomerate structures, not fibrillar structures. *Toxicol Sci*. 2010;113(1):226–242. doi:10.1093/toxsci/kfp247
123. Porter DW, Hubbs AF, Chen BT, et al. Acute pulmonary dose-responses to inhaled multi-walled carbon nanotubes. *Nanotoxicology*. 2013;7(7):1179–1194. doi:10.3109/17435390.2012.719649
124. Ryman-Rasmussen JP, Cesta MF, Brody AR, et al. Inhaled carbon nanotubes reach the subpleural tissue in mice. *Nat Nanotechnol*. 2009;4(11):747–751. doi:10.1038/nnano.2009.305
125. Ma-Hock L, Treumann S, Strauss V, et al. Inhalation toxicity of multiwall carbon nanotubes in rats exposed for 3 months. *Toxicol Sci*. 2009;112(2):468–481. doi:10.1093/toxsci/kfp146
126. Mercer RR, Scabilloni JF, Hubbs AF, et al. Distribution and fibrotic response following inhalation exposure to multi-walled carbon nanotubes. *Part Fibre Toxicol*. 2013;10:33. doi:10.1186/1743-8977-10-33

127. Shvedova AA, Kisin E, Murray AR, et al. Inhalation vs aspiration of single-walled carbon nanotubes in C57BL/6 mice: inflammation, fibrosis, oxidative stress, and mutagenesis. *Am J Physiol*. 2008;295(4):L552–565. doi:10.1152/ajplung.90287.2008
128. Kagan VE, Konduru NV, Feng W, et al. Carbon nanotubes degraded by neutrophil myeloperoxidase induce less pulmonary inflammation. *Nat Nanotechnol*. 2010;5(5):354–359. doi:10.1038/nnano.2010.44
129. Ding Y, Tian R, Yang Z, Chen J, Lu N. NADPH oxidase-dependent degradation of single-walled carbon nanotubes in macrophages. *J Mater Sci*. 2017;28(1):1–8. doi:10.1007/s10856-016-5790-6
130. Kotchey GP, Zhao Y, Kagan VE, Star A. Peroxidase-mediated biodegradation of carbon nanotubes in vitro and in vivo. *Adv Drug Deliv Rev*. 2013;65(15):1921–1932. doi:10.1016/j.addr.2013.07.007
131. Yuan X, Zhang X, Sun L, Wei Y, Wei X. Cellular toxicity and immunological effects of carbon-based nanomaterials. *Part Fibre Toxicol*. 2019;16(1):18. doi:10.1186/s12989-019-0299-z
132. Guzmán-Mendoza J, Montes-Fonseca SL, Ramos-Martínez E, et al. Safe administration of carbon nanotubes by intravenous pathway in BALB/c mice. *Nanomaterials*. 2020;10(2):400. doi:10.3390/nano10020400

International Journal of Nanomedicine

Dovepress

## Publish your work in this journal

The International Journal of Nanomedicine is an international, peer-reviewed journal focusing on the application of nanotechnology in diagnostics, therapeutics, and drug delivery systems throughout the biomedical field. This journal is indexed on PubMed Central, MedLine, CAS, SciSearch®, Current Contents®/Clinical Medicine, Journal Citation Reports/Science Edition, EMBase, Scopus and the Elsevier Bibliographic databases. The manuscript management system is completely online and includes a very quick and fair peer-review system, which is all easy to use. Visit <http://www.dovepress.com/testimonials.php> to read real quotes from published authors.

Submit your manuscript here: <https://www.dovepress.com/international-journal-of-nanomedicine-journal>